JOURNAL OF COMPUTATIONAL PHYSICS **138,** 354–399 (1997)
ARTICLE NO. CP975838

An Evaluation of Roe's Scheme Generalizations for Equilibrium Real Gas Flows

Lorenzo Mottura, Luigi Vigevano, and Marco Zaccanti[1]

Dipartimento di Ingegneria Aerospaziale, Politecnico di Milano, Via Golgi 40, 20133 Milan, Italy
E-mail: vigevano@aero.polimi.it

Received May 9, 1996; revised February 12, 1997

The extension of Roe's approximate Riemann solver to equilibrium real gas is analyzed by means of a general formulation, allowing us to clarify the inherent nonuniqueness of the average state and the influence of the functional form of the equation of state. Several generalizations of Roe's scheme are then reviewed and their numerical performances are discussed by computing some 2D steady hypersonic flows. The flow solvers are coupled with a newly developed, efficient, and robust procedure for thermochemical air properties evaluation. All of the tested equilibrium solvers achieve very similar results. They are found of comparable numerical efficiency, the higher performances being associated with Vinokur's and Liou's solvers. It is concluded that equilibrium simulations in 2D are by no means less robust than the perfect gas ones, when coupled with the proposed procedure for properties evaluation.

Key Words: equilibrium real gas; flux difference splitting.

1. INTRODUCTION

In hypersonic flight regimes, typical of atmosphere reentries or suborbital flights, most of the kinetic energy of the flow surrounding the aircraft is converted to internal energy through the strong bow shock, thus increasing the temperature enormously. As the temperature increases, air can be considered neither as a calorically perfect gas, because of the activation of vibrational energy that depends nonlinearly with temperature, nor as a thermally perfect gas, since chemical reactions alter the mixture composition.

[1] Current address: Mississippi State University/E.R.C. for Computational Field Simulation, P.O. Box A, Mississippi State, MS 39762.

0021-9991/97 $25.00

The most general way of treating high temperature gases requires accounting for both thermal and chemical nonequilibrium. However, nonequilibrium numerical simulations are very demanding in terms of computational resources. Introducing the assumption of local equilibrium allows one to perform hypersonic flow simulations at a much lower cost. Some indications on the applicability of the equilibrium hypothesis may be derived from typical flight paths on a velocity–altitude map [1]. At sufficiently low altitudes and low speeds, the assumption of local thermochemical equilibrium can be considered valid; thus, equilibrium calculations are often sufficient to give correct results in many hypersonic flows of practical interest.

The approaches to equilibrium flow simulation proposed in recent years differ in terms of both physical modeling and numerical methods, many of them being based on flux vector or flux difference splitting upwind schemes [2–10]. After these developments, very few evaluations of the different schemes have been attempted; see [11] for 1D flow and [12] for 2D flow. Among the various upwind methods, one of the most popular is the Roe's scheme, which was originally proposed for a perfect gas [13]. Its main feature is that the upwind formulation is obtained introducing and solving exactly a set of Riemann problems over the linearized system of conservation laws; in this way the resulting scheme attains both high accuracy and good numerical efficiency.

The generalization of Roe's approximate Riemann solver (ARS) to real gas at equilibrium conditions may follow different approaches; the so-called Roe-average state, at which the local linearization is performed, is not uniquely defined, thus allowing for different definitions of some of the average variables. In addition, different thermodynamic quantities may be selected as independent variables in the equation of state for the pressure, influencing the number of average variables to be defined. For these reasons, several extensions of Roe's ARS to equilibrium gas flows have been attempted [4–10] and they can roughly be divided into three families. In the first family [4] an equivalent-γ approach is utilized, trying in some way to remain in a perfect-gas framework by making suitable approximations. The algorithms of the second family [5–7], instead, follow a more consistent approach by including the pressure-derivative terms in the Jacobian matrix exactly. This latter procedure leads to the definition of a Roe-average state based on a more sound theoretical background than the former. Only Vinokur's algorithm [5], however, has been numerically tested for 2D problems [12]. In the third family, a slightly different approach is followed [8–10], which includes explicitly the dependence of the pressure derivatives on the mixture composition.

One of the purposes of this paper is to evaluate and discuss the differences between the various existing generalizations of Roe's scheme to equilibrium flows, and to understand how the different formulations affect the numerical results and the computational efficiency over some 2D equilibrium hypersonic flows of practical significance. Since our interest is focused on upwind differencing of the inviscid terms, we restrict ourselves to the Euler equations.

When determining the approximate solution of the Riemann problem at the control volume interfaces, particular care has to be devoted to the calculation of the thermodynamic state of the mixture. The composition and thermophysical properties of dissociating and ionizing air have been curve-fitted for a wide range

of state variables [14], but although curve-fit calculations may be very competitive in terms of computational requirements, they can lead in some occasions to an unphysical Roe-averaged state, negatively affecting the convergence. The second purpose of this paper is therefore to present a robust and accurate methodology to compute the equilibrium properties of air via chemical composition determination; moreover, we show that this can be done with an acceptable additional computational cost with respect to the use of curve-fits.

This paper is divided in two parts. In the first part (Section 2) we present the newly developed, robust methodology to compute equilibrium properties of air as applied to different air models of increasing complexity. In the second part, we first develop a very general formulation of Roe's ARS for equilibrium real gas (Section 3). Then in Section 4, we analyze and discuss some of the proposed extensions of Roe's scheme. Finally, in Section 5 we present results obtained over typical blunt body and double ellipse configurations, in order to assess the capability of the various methods in predicting 2D equilibrium steady flows.

2. EVALUATION OF EQUILIBRIUM THERMOCHEMICAL PROPERTIES

If the flow is assumed to be in local thermochemical equilibrium, then it follows from thermodynamic considerations that its local properties are a function of only two independent state variables. Therefore, no further differential equation has to be added to the Euler system and the gas properties may be evaluated through a procedure decoupled from the flow solver. In this section we present a procedure of this kind, specifically aimed at being employed in hypersonic flow field calculations. We will follow an approach somewhat similar to the one proposed in [15], the main difference being the method of solution of the nonlinear algebraic system that arises from the equations governing an equilibrium mixture of gases. Due to the system stiffness, particular care is required in order to prevent the solution from blowing up and to force it to converge to the correct physical solution; since in our experience the fixes proposed in the literature [19, 20] were found to be unsatisfactory, we suggest a new approach which proved to be both robust and computationally efficient.

2.1. Thermochemical Equilibrium Model

In the following we will consider the air as a mixture of N_C chemical species, each behaving as a thermally perfect gas. The thermodynamic properties of a mixture of gases can be expressed as functions of those of the single species; we briefly recall here the corresponding equations of state for completeness.

The internal energy per unit mass of the gas mixture is

$$e = e(T, \{\rho_s\}) = \sum_{s=1}^{N_C} \frac{\rho_s}{\rho} e_s(T), \tag{1}$$

where ρ_s and $e_s(T)$ are respectively the density and internal energy per unit mass of species s,

$$\rho = \sum_{s=1}^{N_C} \rho_s \tag{2}$$

being the density, and T the equilibrium temperature of the mixture. The internal energy per unit mass of a diatomic thermally perfect gas can be expressed as the sum of its translational, rotational, vibrational, and electronic energy and of its heat of formation [16],

$$e_s(T) = \frac{5}{2} R_s T + \frac{R_s \Theta_s}{e^{\Theta_s/T} - 1} + e_{\mathrm{el},s} + \Delta h_s^{\mathrm{f}}, \tag{3}$$

where the vibrational contribution has been approximated by means of a simple harmonic oscillator, with Θ_s representing the characteristic vibrational temperature of the molecule considered. This approximation is valid in most cases of practical interest; moreover, the electronic contribution can usually be neglected. The single species constant R_s is given by $R_s = \hat{R}/m_s$, where $\hat{R}$ is the universal constant of gases and m_s is the molar mass of species s.

For a monatomic gas the following relation holds instead of (3):

$$e_s(T) = \frac{3}{2} R_s T + e_{\mathrm{el},s} + \Delta h_s^{\mathrm{f}}, \tag{4}$$

where again the electronic energy can be neglected; similarly, for the free electron

$$e_s(T) = \tfrac{3}{2} R_s T + \Delta h_s^{\mathrm{f}} \quad (s = \text{electron}). \tag{5}$$

The pressure P may be obtained using the thermal equation of state for the single chemical component and Dalton's law,

$$P = P(T, \{\rho_s\}) = \sum_{s=1}^{N_C} \rho_s R_s T = \rho R T, \tag{6}$$

where

$$R = R(\{\rho_s\}) = \sum_{s=1}^{N_C} \frac{\rho_s}{\rho} R_s. \tag{7}$$

The mixture specific enthalpy is immediately determined as

$$h = h(T, \{\rho_s\}) = e + P/\rho = e(T, \{\rho_s\}) + R(\{\rho_s\})T. \tag{8}$$

The speed of sound is expressed in different forms according to which independent variables are chosen for the pressure function, as shown in Section 4.

The thermodynamic properties of the mixture depend upon the temperature and chemical composition. In equilibrium conditions, both T and $\{\rho_s\}$ depend on only two thermodynamic variables; in particular, having in mind the coupling with the

Euler equations, we assume the dependence to be on density and internal energy per unit volume, ε. The thermochemical state of the mixture thus can be determined by solving a nonlinear system of $N_C + 1$ algebraic equations in the $N_C + 1$ unknowns $\{\rho_s\}$ and T. Let us assume that the chemical species of the mixture involve a number of N_E distinct atomic elements, among which we also include the free electron when dealing with ionized species. Then, the equations to be considered are N_E mass (and charge) conservation equations, $N_C - N_E$ equations expressing the Law of Mass Action applied to a set of independent chemical reactions, and the energy equation. To formulate the resulting system in a general way, independently from the selected kinetic model, we will denote each atomic element by ${}^iZ$, $i = 1, ..., N_E$, so that the general formula of the sth species reads

$$X_s = {}^1Z_{a_{s,1}} \ldots {}^iZ_{a_{s,i}} \ldots {}^{N_E}Z_{a_{s,N_E}}, \tag{9}$$

where all $a_{s,i}$ are integers that specify the number of atoms of element i present in species s. The generic jth chemical reaction may then be expressed as

$$\sum_{s=1}^{N_C} \nu'_{s,j} X_s \Leftrightarrow \sum_{s=1}^{N_C} \nu''_{s,j} X_s, \tag{10}$$

where $\nu'_{s,j}$ and $\nu''_{s,j}$ are respectively the stoichiometric coefficients of the reactants and products of species s in the considered reaction.

The equations that define the equilibrium state are therefore [15–16]:

• N_E nuclei and charge conservation equations, N_E being the number of elements which are conserved,

$$\sum_{s=1}^{N_C} \frac{a_{s,i}}{m_s} \frac{\rho_s}{\rho} = \left[\sum_{s=1}^{N_C} \frac{a_{s,i}}{m_s} \frac{\rho_s}{\rho} \right]_{t=t_0}, \quad i = 1, ..., N_E, \tag{11}$$

where the right-hand expression indicates a known composition at a fixed time;

• $N_C - N_E$ equilibrium equations derived from the corresponding set of independent equilibrated chemical reactions,

$$K_j = \frac{\prod_{s=1}^{N_C} (\rho_s/m_s)^{\nu''_{s,j}}}{\prod_{s=1}^{N_C} (\rho_s/m_s)^{\nu'_{s,j}}}, \quad j = 1, ..., N_C - N_E, \tag{12}$$

where $K_j = K_j(T)$ is the equilibrium constant of the jth reaction;

• the equation for the internal energy per unit volume,

$$\varepsilon = \varepsilon(T, \{\rho_s\}) = \rho e = \sum_{s=1}^{N_C} \rho_s \left(n_s R_s T + \frac{R_s \Theta_s}{e^{\Theta_s/T} - 1} + \Delta h_s^f \right), \tag{13}$$

where n_s is equal to $\frac{5}{2}$ for a diatomic gas and $\frac{3}{2}$ for a monatomic gas and the free electron, for which there is no vibrational term.

2.2. Air Chemistry Models

To apply the relations developed in the last section to air, which comprises chemical species containing only oxygen and nitrogen elements, we consider the three following mixtures:

- *Air mixture* 1 (AM1) is made up by the species

$$O_2, N_2, O, N, NO$$

which combine according to the following reactions:

$$O_2 \Leftrightarrow O + O \tag{14}$$

$$N_2 \Leftrightarrow N + N \tag{15}$$

$$NO \Leftrightarrow N + O; \tag{16}$$

- *Air mixture* 2 (AM2) comprises also one ionized species and the free electron,

$$O_2, N_2, O, N, NO, NO^+, e^-,$$

and has the additional ionization reaction:

$$NO \Leftrightarrow NO^+ + e^-; \tag{17}$$

- *Air mixture* 3 (AM3) is composed of the species

$$O_2, N_2, O, N, NO, NO^+, O_2^+, N_2^+, O^+, N^+, e^-,$$

and is characterized by the presence of the following further reactions:

$$O + O \Leftrightarrow O_2^+ + e^- \tag{18}$$

$$N + N \Leftrightarrow N_2^+ + e^- \tag{19}$$

$$O \Leftrightarrow O^+ + e^- \tag{20}$$

$$N \Leftrightarrow N^+ + e^-. \tag{21}$$

The equilibrium constants curve-fits utilized in this work are those given in [17], where they are expressed in moles per cubic centimeter or in a nondimensional form. Vibrational temperatures are taken again from [17], while molar masses and heats of formation are taken respectively from [18, 1]. Moreover, the standard air conditions we have assumed are

$$\rho_0 = 1.225\ \text{kg/m}^3, \quad T_0 = 288.16\ \text{K},$$
$$\eta_{O_2} = 7.35\ \text{mol/kg}, \quad \eta_{N_2} = 27.30\ \text{mol/kg},$$

where $\eta_s = (\rho_s/\rho)/m_s$.

2.3. Solution Methodology

To solve the nonlinear algebraic system arising from Eqs. (11)–(13), applied to the air mixtures reported in the previous section, one can use a Newton–Raphson linearization with the matrix inversion performed, for example, by means of a LU decomposition. However, due to the strong differences in the magnitudes of the terms present in the system, if one applies this method directly, the convergence to the physical solution (the only one with positive partial densities and temperature) is found to be achieved only rarely, even if the initial guess is close to the final solution, and often the iteration is found to explode.

It is therefore necessary to make some modifications in the solution method to attain a robust procedure. By ''robust'' we mean that the procedure must be able to converge starting from virtually any initial guess on temperature and species composition as well as for any given value of internal energy and density. Since the thermochemical solver has to be employed in conjunction with the flow solver, which provides the values of internal energy and density for every grid cell at each time step, robustness is mandatory. In fact, the conditions in each cell may vary significantly at some time step, for example, when a shock front passes through the cell.

To achieve the required robustness, we have experimented with the methods proposed by Cinnella and Cox [19] and by Meintjes and Morgan [20]. The former approach [19] is based on a modified Newton–Raphson method, where a local limitation of the partial densities correction is introduced to avoid convergence to nonphysical solutions. Our implementation of this method does not always guarantee convergence, although it represents a noticeable improvement over the standard Newton–Raphson iteration. The second approach [20] makes use of a global scaling procedure of a reduced system at each iteration and adopts the *absolute Newton–Raphson method*, which consists of taking the absolute value of the increment of the unknowns when updating the solution in the Newton–Raphson linearization. It allows reaching the physical solution for every pair of internal energy and density values of practical interest, starting from virtually every initial guess of partial densities and temperature, but with a rather high computational cost. This is due to the large number of function evaluations necessary to perform the scaling and to the large number of iterations necessary to achieve convergence. For instance, we have reported up to 350 iterations to achieve convergence for AM1, starting from undissociated conditions at some values of density and internal energy.

The interesting concept underlying the scaling procedure is to achieve a reduction of the disparities of magnitude in the terms present in the system. Rather than performing a global scaling of the equations, unknowns and their coefficients at each iteration of the Newton–Raphson loop, we propose an alternative method that first analyzes the problem to identify which are the equations leading to the

numerical instability and then scales the equations and the variables once and for all in a suitable way. This has the advantage of requiring less operations at each iteration, significantly reducing the overall cost of the thermochemical procedure; the price to be paid is only a very limited additional analytical work needed to identify the causes of the convergence difficulty.

Considering reaction (16), one can notice that the formation of NO molecules depends only upon the dissociation of O_2 and N_2, Eqs. (14)–(15). These reactions, at low energy, are completely shifted toward undissociated molecules, causing numerical problems because of the low concentration of NO, O, and N. Actually, it is N that causes most of the difficulties, since dissociation of N_2 molecule begins at a higher temperature than dissociation of O_2 (respectively, at temperature values around 4000 K and 2000 K, almost independently of the density).

To overcome such a difficulty, we propose introducing a set of independent chemical reactions slightly different from (but equivalent to) that described in (14)–(21), with the aim of making the NO formation, as well as that of all the other species, depend upon the dissociation of O_2 and N_2 more directly. Having in mind the most complex mixture, i.e., AM3, the modified chemical reactions we consider are the following:

$$\tfrac{1}{2}O_2 \Leftrightarrow O \tag{22}$$

$$\tfrac{1}{2}N_2 \Leftrightarrow N \tag{23}$$

$$\tfrac{1}{2}O_2 + \tfrac{1}{2}N_2 \Leftrightarrow NO \tag{24}$$

$$\tfrac{1}{2}O_2 + \tfrac{1}{2}N_2 \Leftrightarrow NO^+ + e^- \tag{25}$$

$$O_2 \Leftrightarrow O_2^+ + e^- \tag{26}$$

$$N_2 \Leftrightarrow N_2^+ + e^- \tag{27}$$

$$\tfrac{1}{2}O_2 \Leftrightarrow O^+ + e^- \tag{28}$$

$$\tfrac{1}{2}N_2 \Leftrightarrow N^+ + e^-. \tag{29}$$

Furthermore, besides the temperature, we adopt the unknowns

$$x_s = \sqrt{\rho_s/m_s}, \quad s = 1, 2, \tag{30}$$

$$x_s = \rho_s/m_s, \qquad s = 3, ..., N_C, \tag{31}$$

where partial densities are ordered as in AM3, the first two species being O_2 and N_2. Dividing partial densities by molar masses (expressed in kg/mol) has the advantage of smoothing the differences in the magnitudes of the variables, including temperature. Moreover, using relations (30), besides reducing the magnitude of the equilibrium constants of reactions (22) and (23), makes all of the square roots of the system disappear. The square roots, in fact, would be present in the denominator in some terms of the Jacobian matrix, thus causing difficulties at high temperatures, where the concentrations of O_2 and N_2 are approaching zero. For the solution of the resulting system, the *absolute Newton–Raphson method* [20] has been used, since this method has proved to be more robust than the limiter approach [19].

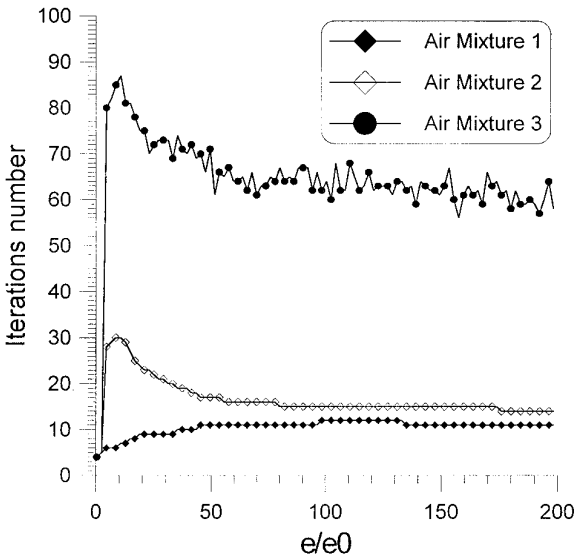

FIG. 1. Number of iterations for the three mixtures versus internal energy per unit mass starting from standard conditions at $\rho = \rho_0$.

In this manner, we have achieved convergence for every pair of density and internal energy values of practical interest with a significant saving of iterations and computational time with respect to the scaling method of Meintjes and Morgan. Although the number of equations and, thus, the order of the matrix is bigger in our system than in [20], function evaluations are much simpler, their number is smaller, and the convergence rate is significantly higher. In order to demonstrate the robustness achieved by the proposed methodology, we have also experimented with the challenging convergence tests presented in [19] for air dissociation and ionization. While the methods proposed in [19] did not always guarantee convergence, as is clearly stressed by the authors, our procedure never failed to converge to the correct physical solution in any of the suggested cases. This gives further confidence in the proposed procedure, in view of its coupling with the flow solver.

Figure 1 presents the number of iterations necessary to reach convergence for the three air mixtures at $\rho = \rho_0$, starting from an undissociated mixture at standard temperature. One can note, in the interval of energies of practical interest that AM3 requires the maximum number of iterations, which is never bigger than 87; however, for the other two air mixtures this number is substantially smaller. In Figs. 2 and 3, the number of iterations for $\rho = 10^{-2}\,\rho_0$ and $\rho = 10^{-4}\,\rho_0$, respectively, are reported, in order to show that for values of density of practical interest the maximum number of iterations of AM3 becomes of the same order of magnitude of that of the simpler mixtures. Analyzing all the three graphs, one can finally note that AM1, which is sufficient to provide the correct thermodynamic properties of air in most cases of practical interest, never needs more than 16 iterations to reach convergence, thus being the most efficient computationally.

If one starts, instead, from an initial guess close enough to the final solution, it has been found that usually no more than five iterations are necessary to achieve

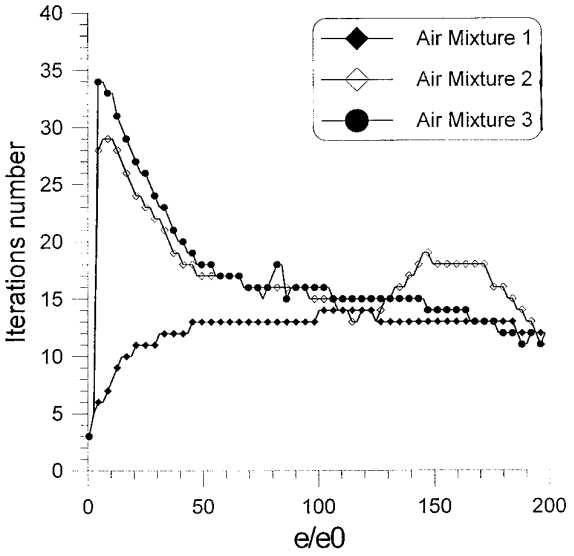

FIG. 2. Number of iterations for the three mixtures versus internal energy per unit mass starting from standard conditions at $\rho = 10^{-2}\ \rho_0$.

convergence for each of the three mixtures. This is particularly important in view of the coupling between the thermochemical procedure and the flow solver, since most of the flow field does not experiment a strong variation during the time-marching procedure.

As an example of the capabilities of our method of computing the correct physical

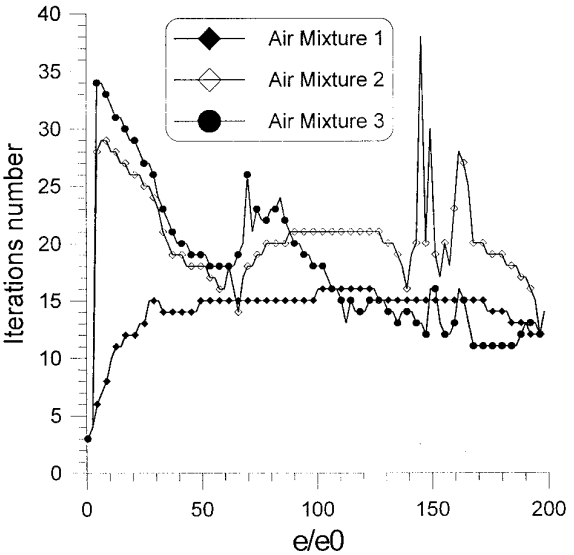

FIG. 3. Number of iterations for the three mixtures versus internal energy per unit mass starting from standard conditions at $\rho = 10^{-4}\ \rho_0$.

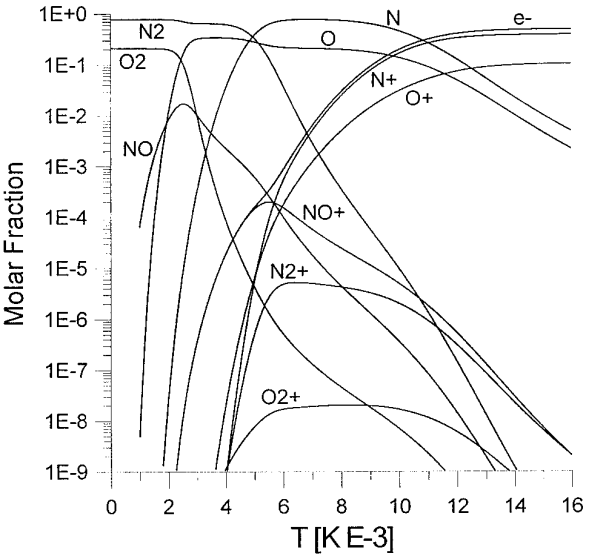

FIG. 4. Chemical composition (AM3) versus temperature at $\rho = 10^{-4}\,\rho_0$.

solution, the chemical composition of AM3 against temperature at the constant density $\rho = 10^{-4}\,\rho_0$ is shown in Fig. 4; other examples are reported in [21].

Once the temperature and chemical composition of the mixture are obtained, all of the other thermodynamic properties of air are easily computed from (1)–(8). The pressure derivatives and the mass fractions derivatives, needed in the evaluation of the speed of sound, must, however, be evaluated by means of the implicit function theorem, the explicit functional dependence of $P = P(\rho, \varepsilon)$ and $\rho_s = \rho_s(\rho, \varepsilon)$ upon ρ and ε being not available. To compute the partial derivatives of pressure with respect to the internal energy per unit volume and density, it is convenient to express them as a function of other thermodynamic derivatives more easily obtainable, such as

$$\left(\frac{\partial P}{\partial \rho}\right)_{\varepsilon} = \left(\frac{\partial T}{\partial \rho}\right)_{\varepsilon} \rho R + T \sum_{s=1}^{N_C} \left(\frac{\partial \rho_s}{\partial \rho}\right)_{\varepsilon} R_s, \tag{32}$$

$$\left(\frac{\partial P}{\partial \varepsilon}\right)_{\rho} = \left(\frac{\partial T}{\partial \varepsilon}\right)_{\rho} \rho R + T \sum_{s=1}^{N_C} \left(\frac{\partial \rho_s}{\partial \varepsilon}\right)_{\rho} R_s. \tag{33}$$

Although the explicit dependence of T and $\{\rho_s\}$ upon ρ and ε is not known, the system of Eqs. (11)–(13), which can be expressed compactly in the vector form

$$\mathbf{f}(\rho, \varepsilon, T, \{\rho_s\}) = 0, \quad \mathbf{f} \in \Re^{N_C+1},$$

implicitly defines the $N_C + 1$ functions $\rho_s = \rho_s(\rho, \varepsilon)$ and $T = T(\rho, \varepsilon)$. The implicit function theorem states that, if the partial derivatives of the vector $\mathbf{f}$ exist and are continuous and if the Jacobian matrix of $\mathbf{f}$, $[\partial \mathbf{f}/\partial(T, \{\rho_s\})]$, is not singular, then the derivatives of T and $\{\rho_s\}$ with respect to ρ and ε are given by

$$\left(\frac{\partial(T,\{\rho_s\})}{\partial\rho}\right)_\varepsilon = -\left[\frac{\partial\mathbf{f}}{\partial(T,\{\rho_s\})}\right]^{-1}\left(\frac{\partial\mathbf{f}}{\partial\rho}\right)_\varepsilon \tag{34}$$

$$\left(\frac{\partial(T,\{\rho_s\})}{\partial\varepsilon}\right)_\rho = -\left[\frac{\partial\mathbf{f}}{\partial(T,\{\rho_s\})}\right]^{-1}\left(\frac{\partial\mathbf{f}}{\partial\varepsilon}\right)_\rho. \tag{35}$$

Equations (34) and (35) give the solution of two linear algebraic systems with the same coefficient matrix of the original Newton–Raphson loop. It is also possible to write the problem in a slightly different way, making use of the Jacobian of the modified system we proposed, so that again the same matrix can be utilized in both the loop and the determination of the implicitly defined variables.

3. GENERALIZATION OF ROE'S SCHEME TO EQUILIBRIUM REAL GAS

In this section we will present a general form of the extension of Roe's ARS to real gas at equilibrium conditions, in order to set a framework in which the schemes [4–8] developed by different authors may be evaluated. The three schemes, that will be evaluated numerically, will then be described in more detail in the next section.

For the sake of simplicity, we will restrict the discussion to the 1D case; in this way, the main properties of the various approaches can be easily highlighted without losing generality. Selected schemes have then been applied to 2D flows through a finite volume approach and an assumption of local monodimensionality.

The Euler equations in one space dimension can be written in conservative form as

$$\frac{\partial u}{\partial t} + \frac{\partial f}{\partial x} = 0, \tag{36}$$

where the vector of the conservative variables and the flux vector are given respectively by

$$u = \begin{Bmatrix} \rho \\ m \\ E \end{Bmatrix}, \quad f(u) = \begin{Bmatrix} m \\ m^2/\rho + P \\ (E+P)m/\rho \end{Bmatrix}, \tag{37}$$

where $m = \rho v$ is the momentum per unit volume, v is the velocity, and E is the total energy per unit volume:

$$E = \rho e + \tfrac{1}{2}\rho v^2 = \varepsilon + \tfrac{1}{2}\rho v^2. \tag{38}$$

The flux Jacobian matrix $A(u) = \partial f/\partial u$ may be written in the most general form by considering the pressure P as a function of the conservative variables,

$$P = \Pi(\rho, m, E). \tag{39}$$

Equation (39) is not a thermodynamic relation; for a gas in equilibrium conditions, pressure is a function of only two independent variables. Equation (39) represents, however, a very convenient functional form to generalize Roe's scheme for a gas with an arbitrary equation of state.

It follows that

$$A(u) = \begin{bmatrix} 0 & 1 & 0 \\ \Pi_\rho - v^2 & \Pi_m + 2v & \Pi_E \\ (\Pi_\rho - H)v & H + \Pi_m v & (1 + \Pi_E)v \end{bmatrix}, \tag{40}$$

where $H = h + \frac{1}{2}v^2$ represents the total enthalpy per unit mass. We now introduce the auxiliary vector

$$\omega(u) = (v, H, \Pi_\rho, \Pi_m, \Pi_E)^{\mathrm{T}}, \tag{41}$$

to indicate the explicit occurrence in the Jacobian matrix of the variables v, H, as well as of the pressure derivatives,

$$\Pi_\rho = \left(\frac{\partial \Pi}{\partial \rho}\right)_{m,E}, \quad \Pi_m = \left(\frac{\partial \Pi}{\partial m}\right)_{\rho,E}, \quad \Pi_E = \left(\frac{\partial \Pi}{\partial E}\right)_{\rho,m}, \tag{42}$$

the latter satisfying the differential relation:

$$dP = \Pi_\rho \, d\rho + \Pi_m \, dm + \Pi_E \, dE. \tag{43}$$

With this notation the Jacobian can also be viewed as a function of ω, according to the definition:

$$A(u) = {}_A(\omega(u)) = {}_A(\omega). \tag{44}$$

Finally, in this framework the speed of sound is given by

$$a^2 = \Pi_\rho + (H - v^2)\Pi_E. \tag{45}$$

3.1. Roe's Approximate Riemann Solver for a Perfect Gas

Roe's ARS is based on a local linearization of the governing equations

$$\frac{\partial u}{\partial t} + \tilde{A} \frac{\partial u}{\partial x} = 0 \tag{46}$$

at each cell interface. The Riemann problem defined by the linear equation (46) and the discontinuous initial condition u_{L}, u_{R} across the interface is then solved exactly. Matrix $\tilde{A} = \tilde{A}(u_{\mathrm{L}}, u_{\mathrm{R}})$ is defined by the following set of properties, christened by Roe as "Property U":

(i) $\tilde{A}(u_{\mathrm{L}}, u_{\mathrm{R}})$ constitutes a linear mapping from the vector space u to the vector space f;

(ii) $\tilde{A}(u_{\mathrm{L}}, u_{\mathrm{R}}) \to A(u)$ as $u_{\mathrm{L}} \to u_{\mathrm{R}} \to u$;

(iii) $\tilde{A}(u_{\mathrm{L}}, u_{\mathrm{R}})$ has linearly independent eigenvectors;

(iv) $\tilde{A}(u_{\mathrm{L}}, u_{\mathrm{R}})$ must satisfy the relation:

$$\Delta f = \tilde{A}(u_{\mathrm{L}}, u_{\mathrm{R}}) \, \Delta u, \tag{47}$$

where the operator $\Delta(\cdot) = (\cdot)_R - (\cdot)_L$ represents the jump in the quantity $(\cdot)$ across the interface between left and right states.

Property (iv) is a sufficient condition to have a conservative method and assures, together with property (iii), that shock waves are handled exactly. It is actually used for the algebraic derivation of $\tilde{A}$.

Using a parameter vector technique, Roe derived the matrix $\tilde{A}$ for a perfect gas as

$$\tilde{A} = {}_A(\tilde{z}), \tag{48}$$

where the so-called Roe-average state $\tilde{z} \equiv \tilde{z}_{PG} = (\tilde{v}, \tilde{H})^T$ is uniquely defined by

$$\tilde{v} = \mathrm{Ro}(v), \tag{49}$$

$$\tilde{H} = \mathrm{Ro}(H), \tag{50}$$

with the Roe-average operator defined as

$$\mathrm{Ro}(\cdot) = \frac{\sqrt{\rho_L}(\cdot)_L + \sqrt{\rho_R}(\cdot)_R}{\sqrt{\rho_L} + \sqrt{\rho_R}}. \tag{51}$$

The chosen notation intends to emphasize that the average state implies only those variables that explicitly appear in the Jacobian matrix. It is easy to check that Eq. (48), obtained by satisfying property (iv), meets all of the other requirements set by Property U.

Roe's original result has been utilized by several authors to achieve a simpler way of determining $\tilde{A}$. If one *assumes* that Eq. (48) holds, it is possible to look immediately for the average state $\tilde{z}$ that satisfies property (iv) by direct substitution in Eq. (47) or in the eigenvector expansion of Δf and Δu. When dealing with a perfect gas the three approaches, namely,

(a) using parameter vectors,

(b) assuming Eq. (48) and using direct substitution in Eq. (47),

(c) assuming Eq. (48) and using direct substitution in the eigenvector expansion of Δf and Δu

lead, obviously, to the definition of the same average state $\tilde{z}$ and matrix $\tilde{A}$.

3.2. Determination of Roe's Average State for a Real Gas

When considering a real gas obeying a general equation of state, the above result has not been proven. Most of the proposed formulations [5–8] extrapolate Roe's perfect gas result and assume as the starting point Eq. (48), arriving at different formulas depending upon which approach—(b) or (c)—and which independent thermodynamic variables are selected. The single attempt [4] of using approach (a), due to the introduction of simplifying hypothesis, has led to a definition of $\tilde{A}$ that does not satisfy Eq. (48).

The problem is complicated by the fact that for a general equation of state for the pressure, the Roe-average state $\tilde{z}$ is sought for the vector ω defined by Eq. (41) and, therefore, is not uniquely defined, because there are less equations than average variables to be defined. In fact the number of components of the auxiliary vector ω exceeds the number of conditions expressed by Eq. (47).

Thus, apparently there are three features that lead to the different generalizations of Roe's scheme in the case of real gases: (i) the way in which the matrix $\tilde{A}$ is derived; (ii) the way in which the pressure is related to the other thermodynamic variables; (iii) the nonuniqueness of the average state. Unfortunately, the precise consequences of each of these features have not been analyzed in the formulations proposed by previous authors. Selecting an equation of state for the pressure at the beginning of the derivation and thus specializing the form of the flux vector (37), the Jacobian (40), and the related eigenvectors has hidden the role played by the technique used to define $\tilde{A}$ and $\tilde{z}$.

The general formulation here adopted, Eqs. (39)–(41), allows us to show that, albeit the average state $\tilde{z}$ is not uniquely defined, all of the three approaches–(a), (b), (c)—described above lead to the same formal definition of $\tilde{A}$, satisfying (47) and (48) and to the same linear constraint for the averages of the pressure derivatives (42). This represents an effective generalization of the result obtained by Roe for the perfect gas case.

In this subsection, we want to demonstrate that, starting from the very general equation of state (39) and the Jacobian (40), all of the techniques outlined above lead to the following definition of $\tilde{A}$ as

$$\tilde{A} = {}_A(\tilde{z}) = \begin{bmatrix} 0 & 1 & 0 \\ \tilde{\Pi}_\rho - \tilde{v}^2 & \tilde{\Pi}_m + 2\tilde{v} & \tilde{\Pi}_E \\ (\tilde{\Pi}_\rho - \tilde{H})\tilde{v} & \tilde{H} + \tilde{\Pi}_m\tilde{v} & (1 + \tilde{\Pi}_E)\tilde{v} \end{bmatrix} \tag{52}$$

with $\tilde{v}$ and $\tilde{H}$ defined by (49)–(50) as in the original Roe's scheme and with the average pressure derivatives satisfying the linear relation

$$\Delta P = \tilde{\Pi}_\rho \Delta\rho + \tilde{\Pi}_m \Delta m + \tilde{\Pi}_E \Delta E \tag{53}$$

that corresponds to the discrete form of Eq. (43), averaged between the two states, and expresses the nonuniqueness of the Roe-average state for a real gas.

3.2.1. *Parameter Vectors*

Selecting as a parameter the vector

$$z = \begin{Bmatrix} \sqrt{\rho} \\ v\sqrt{\rho} \\ H\sqrt{\rho} \end{Bmatrix} = \begin{Bmatrix} z_1 \\ z_2 \\ z_3 \end{Bmatrix}, \tag{54}$$

the variable and flux vectors may be written as

$$u = \begin{Bmatrix} z_1^2 \\ z_1 z_2 \\ z_1 z_3 - P \end{Bmatrix}, \quad f = \begin{Bmatrix} z_1 z_2 \\ z_2^2 + P \\ z_2 z_3 \end{Bmatrix}. \tag{55}$$

Following Roe's original approach, we look for two matrices $B(\bar{z})$ and $C(\bar{z})$, with

$$\bar{z} = \tfrac{1}{2}(z_{\mathrm{R}} + z_{\mathrm{L}}),$$

such as

$$\Delta f = B(\bar{z})\,\Delta z, \quad \Delta u = C(\bar{z})\,\Delta z. \tag{56}$$

From Eq. (47) it follows immediately that

$$\tilde{A} = B(\bar{z})C(\bar{z})^{-1}. \tag{57}$$

The problem here is to express the jump in pressure ΔP in terms of the components of the jump Δz. From the definition of total enthalpy we know that

$$\Delta E = \Delta(\rho H) - \Delta P. \tag{58}$$

Then, assuming that the linear relation (53) holds, we have

$$\Delta P = \frac{1}{1 + \tilde{\Pi}_E}[\tilde{\Pi}_\rho\,\Delta\rho + \tilde{\Pi}_m \Delta(\rho v) + \tilde{\Pi}_E \Delta(\rho H)]. \tag{59}$$

Furthermore, from the definition of the parameter vector z we can derive

$$\Delta\rho = 2\bar{z}_1\,\Delta z_1 \tag{60.a}$$

$$\Delta(\rho v) = \bar{z}_2\,\Delta z_1 + \bar{z}_1\,\Delta z_2 \tag{60.b}$$

$$\Delta(\rho H) = \bar{z}_3\,\Delta z_1 + \bar{z}_1\,\Delta z_3 \tag{60.c}$$

and, hence,

$$\Delta P = \frac{1}{1 + \tilde{\Pi}_E}[(2\bar{z}_1\tilde{\Pi}_\rho + \bar{z}_2\tilde{\Pi}_m + \bar{z}_3\tilde{\Pi}_E)\,\Delta z_1 + \bar{z}_1\tilde{\Pi}_m\,\Delta z_2 + \bar{z}_1\tilde{\Pi}_E\,\Delta z_3]. \tag{61}$$

Having expressed ΔP in terms of the components of the jump Δz, a straightforward calculation leads to

$$B(\overline{z}) = \begin{bmatrix} \overline{z}_2 & \overline{z}_1 & 0 \\ \dfrac{2\overline{z}_1\tilde{\Pi}_\rho + \overline{z}_2\tilde{\Pi}_m + \overline{z}_3\tilde{\Pi}_E}{1+\tilde{\Pi}_E} & 2\overline{z}_2 + \dfrac{\overline{z}_1\tilde{\Pi}_m}{1+\tilde{\Pi}_E} & \dfrac{\overline{z}_1\tilde{\Pi}_E}{1+\tilde{\Pi}_E} \\ 0 & \overline{z}_3 & \overline{z}_2 \end{bmatrix}, \tag{62}$$

$$C(\overline{z}) = \begin{bmatrix} 2\overline{z}_1 & 0 & 0 \\ \overline{z}_2 & \overline{z}_1 & 0 \\ \dfrac{\overline{z}_3 - 2\overline{z}_1\tilde{\Pi}_\rho - \overline{z}_2\tilde{\Pi}_m}{1+\tilde{\Pi}_E} & \dfrac{-\overline{z}_1\tilde{\Pi}_m}{1+\tilde{\Pi}_E} & \dfrac{\overline{z}_1}{1+\tilde{\Pi}_E} \end{bmatrix}. \tag{63}$$

Noting that the ratios

$$\frac{\overline{z}_2}{\overline{z}_1} = \tilde{v}, \quad \frac{\overline{z}_3}{\overline{z}_1} = \tilde{H}$$

represent the usual Roe averages, Eqs. (49) and (50), we can finally substitute (62) and (63) in Eq. (57), leading to the matrix $\tilde{A}$ as given by Eq. (52).

We remark here that using an equation of state in the perfect gas-like form,

$$P = P(\rho, e) = [\gamma(\rho, e) - 1]\rho e,$$

with $\gamma(\rho, e)$ a suitable known function, prevents the above result to be obtained (see for instance [4]). In fact, in this case the expression of the jump ΔP is complicated by the presence of the term $\Delta\gamma$, which cannot be expressed in terms of Δz, and some approximations in the behavior of γ and $\Delta\gamma$ must be introduced. Actually, in [4] the authors consider that $\Delta\gamma$ is related to ΔP via an isentropic formula and that the jumps in γ and the isentropic index,

$$\Gamma = \Gamma(\rho, e) = \frac{\rho a^2}{P},$$

are always very small; moreover, they assume that γ and Γ have nearly the same values. In [5] it is shown that this procedure is equivalent to consider the pressure derivative $(\partial P/\partial\rho)_\varepsilon = 0$, which is not physically justified. Even though the function γ is physically bounded between the values 1 and 1.4, it varies nonmonotonically and a variation in γ may strongly affect the pressure; thus, when the two states are far apart, all of these approximations are inadequate.

3.2.2. *Direct Substitution*

This approach is the most straightforward way of obtaining the Roe's average state. It starts directly from the definition of $\tilde{A}$ as in Eq. (52), to derive the average state $\tilde{u}$ that satisfies Eqs. (47).

Out of the three resulting equations, the first reduces to an identity. The second equation,

$$\Delta(\rho v^2) + \Delta P = (\tilde{\Pi}_\rho - \tilde{v}^2)\,\Delta\rho + (2\tilde{v} + \tilde{\Pi}_m)\,\Delta m + \tilde{\Pi}_E\,\Delta E,$$

may be rewritten as

$$\Delta P = \tilde{\Pi}_\rho\,\Delta\rho + \tilde{\Pi}_m\,\Delta m + \tilde{\Pi}_E\,\Delta E - [\tilde{v}^2\,\Delta\rho - 2\tilde{v}\Delta(\rho v) + \Delta(\rho v^2)]. \tag{64}$$

As for the perfect gas case, it is easy to check that, if $\tilde{v}$ is defined as in Eq. (49), it becomes

$$\tilde{v}^2\,\Delta\rho - 2\tilde{v}\Delta(\rho v) + \Delta(\rho v^2) = 0, \tag{65}$$

so that Eq. (64) reduces to Eq. (53).

The third equation,

$$\Delta(\rho v H) = (\tilde{\Pi}_\rho - \tilde{H})\tilde{v}\,\Delta\rho + (\tilde{H} + \tilde{\Pi}_m\tilde{v})\,\Delta m + (1 + \tilde{\Pi}_E)\tilde{v}\,\Delta E,$$

may be rewritten, using Eq. (58), as

$$\tilde{H}[\tilde{v}\,\Delta\rho - \Delta(\rho v)] = \tilde{v}\Delta(\rho H) - \Delta(\rho v H) + \tilde{v}[\tilde{\Pi}_\rho\,\Delta\rho + \tilde{\Pi}_m\,\Delta m + \tilde{\Pi}_E\,\Delta E - \Delta P]. \tag{66}$$

The last term of the r.h.s. of Eq. (66) vanishes because of Eq. (53). We are left then with

$$[\tilde{v}\,\Delta\rho - \Delta(\rho v)]\tilde{H} = \tilde{v}\Delta(\rho H) - \Delta(\rho v H) \tag{67}$$

that defines $\tilde{H}$ as in Eq. (50).

3.2.3. *Eigenvector Expansion*

Instead of looking directly for $\tilde{A}$, this approach determines the average state $\tilde{w}$ as the one satisfying the eigenvector expansions

$$\Delta f = \sum_{p=1}^{3} \tilde{\beta}_p\,\tilde{\lambda}_p\,\tilde{\mathbf{r}}_p \tag{68}$$

$$\Delta u = \sum_{p=1}^{3} \tilde{\beta}_p\,\tilde{\mathbf{r}}_p, \tag{69}$$

where the $\tilde{\lambda}_p$ are the eigenvalues of matrix $\tilde{A}$ defined by (52), namely,

$$\tilde{\lambda}_1 = \tilde{v}, \quad \tilde{\lambda}_2 = \tilde{v} + \tilde{a}, \quad \tilde{\lambda}_3 = \tilde{v} - \tilde{a}, \tag{70}$$

and $\tilde{\mathbf{r}}_p$ are the corresponding right eigenvectors, which are the columns of the matrix

$$\tilde{R} = \begin{bmatrix} 1 & 1 & 1 \\ \tilde{v} & \tilde{v} + \tilde{a} & \tilde{v} - \tilde{a} \\ \tilde{H} - \dfrac{\tilde{a}^2}{\tilde{\Pi}_E} & \tilde{H} + \tilde{a}\tilde{v} & \tilde{H} - \tilde{a}\tilde{v} \end{bmatrix}. \tag{71}$$

The $\tilde{\beta}_p$ are the wave intensities, components of the vector $\tilde{\beta}$:

$$\tilde{\beta} = \tilde{R}^{-1}\,\Delta u = \begin{Bmatrix} \Delta\rho - \dfrac{\Delta P}{\tilde{a}^2} \\ \dfrac{\Delta P}{2\tilde{a}^2} + \dfrac{1}{2\tilde{a}}\left[\Delta(\rho v) - \tilde{v}\,\Delta\rho\right] \\ \dfrac{\Delta P}{2\tilde{a}^2} - \dfrac{1}{2\tilde{a}}\left[\Delta(\rho v) - \tilde{v}\,\Delta\rho\right] \end{Bmatrix}. \tag{72}$$

The average speed of sound, as defined from the eigenvalue calculation, is

$$\tilde{a}^2 = \tilde{\Pi}_\rho + (\tilde{H} - \tilde{v}^2)\tilde{\Pi}_E. \tag{73}$$

Developing the relations (69), it is easy to check that the first and the second reduce to an identity. The third relation becomes

$$\Delta E = \left(\tilde{H} - \tilde{v}^2 - \frac{\tilde{a}^2}{\tilde{\Pi}_E}\right)\Delta\rho + \tilde{v}\Delta(\rho v) + \frac{\Delta P}{\tilde{\Pi}_E}; \tag{74}$$

using the definition (73) it becomes

$$\Delta P = \tilde{\Pi}_\rho\,\Delta\rho - \tilde{v}\tilde{\Pi}_E\,\Delta m + \Pi_E\,\Delta E. \tag{75}$$

Equation (75) is equivalent to the linear relation (53) if

$$\tilde{\Pi}_m = -\tilde{v}\tilde{\Pi}_E. \tag{76}$$

Equation (76) formally constitutes an additional constraint on the average pressure derivatives to be added to Eq. (53). It will be shown, however, that since the corresponding relation between pressure derivatives is satisfied pointwise (at left and right states), due to thermodynamic equivalencies, Eq. (76) is always satisfied for any equation of state.

Turning now to the relations (68), the first again gives an identity. The second relation becomes equal to Eq. (65) and, hence, defines $\tilde{v}$ as in Eq. (49). Finally, the third relation becomes

$$\Delta(\rho v H) = -\tilde{v}\left(\tilde{v}^2 + \frac{\tilde{a}^2}{\tilde{\Pi}_E}\right)\Delta\rho + \tilde{v}\left(1 + \frac{1}{\tilde{\Pi}_E}\right)\Delta P + (\tilde{H} + \tilde{v}^2)\Delta(\rho v). \tag{77}$$

Using again the definition (73), Eq. (77) may be rewritten as

$$\tilde{H}[\Delta(\rho v) - \tilde{v}\Delta\rho] = \Delta(\rho v H) + \tilde{v}\frac{\tilde{\Pi}_\rho}{\tilde{\Pi}_E}\Delta\rho - \tilde{v}\left(1 + \frac{1}{\tilde{\Pi}_E}\right)\Delta P - \tilde{v}^2\Delta(\rho v). \tag{78}$$

Supposing that the linear relation (53) holds and considering Eq. (58), we may write

$$\left(1 + \frac{1}{\tilde{\Pi}_E}\right)\Delta P = \frac{\tilde{\Pi}_\rho}{\tilde{\Pi}_E}\Delta\rho + \frac{\tilde{\Pi}_m}{\tilde{\Pi}_E}\Delta(\rho v) + \Delta(\rho H), \tag{79}$$

so that Eq. (78) reads

$$\tilde{H}[\tilde{v}\Delta\rho - \Delta(\rho v)] = \tilde{v}\Delta(\rho H) - \Delta(\rho v H) + \tilde{v}\left(\tilde{v} + \frac{\tilde{\Pi}_m}{\tilde{\Pi}_E}\right)\Delta(\rho v). \tag{80}$$

Considering Eq. (76), the last term on the r.h.s. vanishes and Eq. (80) reduces to Eq. (67), leading to the definition of $\tilde{H}$ as in Eq. (50).

3.3. Determination of the Generalized Pressure Derivatives

To complete the general formulation proposed here, we need to evaluate the averaged pressure derivatives (42) in terms of the relevant average thermodynamic derivatives according to the selected equation of state. In conditions of local equilibrium, pressure can be related to two other thermodynamic variables through a general equation of state of the form

$$P = \Pi(\rho, m, E) = P(i, \rho), \tag{81}$$

where the variable i can be the internal energy, either per unit mass e or per unit volume ε, or the temperature T. According to which choice is made, the pressure derivatives (42), the auxiliary vector ω (41), and the flux Jacobian matrix (40) will assume a different form, thus influencing the determination of the Roe-average state. It immediately follows that the fewer independent variables are used in the definition of $\tilde{z}$, the fewer averages one must define and, therefore, the number of operations that one has to do is reduced.

The evaluation of the average pressure derivatives (42) may be accomplished with the following steps:

—select an equation of state in the form (81);

—from thermodynamic considerations, derive the relations:

$$\Pi_x = \mathrm{D}\left(\left(\frac{\partial P}{\partial i}\right)_\rho, \left(\frac{\partial P}{\partial \rho}\right)_i, v, e, \rho, \ldots\right), \quad x = \rho, m, E, \tag{82}$$

that satisfy Eq. (43), holding pointwise for any given thermodynamic state;

—assume that the relations (82) carry over for the average values as

$$\tilde{\Pi}_x = \mathrm{D}\left(\left(\frac{\partial \tilde{P}}{\partial i}\right)_\rho, \left(\frac{\partial \tilde{P}}{\partial \rho}\right)_i, \tilde{v}, \tilde{e}, \tilde{p}, \ldots\right), \quad x = \rho, m, E, \tag{83}$$

—insert the relations (83) into Eq. (53) so as to obtain the constraint for the still undefined average variables. In this way, we specialize the nonunique definition of the average state, represented by Eq. (53), to the selected equation of state. Furthermore, since the pointwise relation

$$\Pi_m = -v\Pi_E$$

holds for any equation of state in the form of Eq. (81), the above procedure allows us to always satisfy Eq. (76).

As an example, let us consider a perfect gas for which

$$P = (\gamma - 1)\left(E - \frac{1}{2}\frac{m^2}{\rho}\right) \tag{84}$$

holds. The pressure derivatives are easily computed as

$$\Pi_\rho = \frac{\gamma - 1}{2} v^2, \quad \Pi_m = -(\gamma - 1)v, \quad \Pi_E = \gamma - 1. \tag{85}$$

Supposing the relations (85) hold also for the average values and inserting them into Eq. (53) we obtain

$$\Delta P = \frac{\gamma - 1}{2} \tilde{v}^2 \, \Delta\rho - (\gamma - 1)\tilde{v}\Delta(\rho v) + (\gamma - 1)\, \Delta E. \tag{86}$$

Taking the difference of Eq. (84) and replacing the ΔP term in Eq. (86) gives, finally,

$$\frac{\gamma - 1}{2}[\tilde{v}^2 \, \Delta\rho - 2\tilde{v}\Delta(\rho v) + \Delta(\rho v^2)] = 0,$$

that is identically satisfied because of (65). The above derivation proves that for a perfect gas the Roe-average state expressed by (48) and (49)–(51) is uniquely defined and that the general result given by Eqs. (52)–(53) reduces nicely to the original perfect gas scheme for which Eq. (53) is automatically satisfied.

4. DESCRIPTION OF THE EVALUATED SOLVERS

In this section we will briefly describe the three schemes [5, 7, and 8] that will be evaluated numerically, making use of the general framework developed before. All of them assume as starting point Eq. (48) to define the Roe-average state. The schemes proposed by Vinokur and Montagné [5] and by Liou *et al.* [7] define the

matrix $\tilde{A}$ using direct substitution in Eq. (47)—the approach (b) of the previous section—and differ for the choice of the equation of state and the projection technique formulated to deal with the nonuniqueness of the average state. The scheme proposed by Cox and Cinnella [8] defines the average state using direct substitution in the eigenvector expansions—approach (c)—and does not apply any projection technique.

4.1. Vinokur–Montagné's Generalization

Vinokur and Montagné [5] consider an equation of state of the form

$$P = P(\varepsilon, \rho). \tag{87}$$

I.e., they treat the pressure as a function of internal energy per unit volume and density; using Vinokur's notation, the derivatives of the equation of state are indicated as

$$\kappa = \left(\frac{\partial P}{\partial \varepsilon}\right)_{\rho}, \quad \chi = \left(\frac{\partial P}{\partial \rho}\right)_{\varepsilon}.$$

To obtain the generalized pressure derivatives in form of Eq. (82), let proceed as follows: differencing Eq. (87) we have

$$dP = \kappa\, d\varepsilon + \chi\, d\rho. \tag{88}$$

Then considering $\varepsilon = \varepsilon(\rho, m, E)$ we obtain

$$d\varepsilon = \left(\frac{\partial \varepsilon}{\partial \rho}\right)_{m,E} d\rho + \left(\frac{\partial \varepsilon}{\partial m}\right)_{\rho,E} dm + \left(\frac{\partial \varepsilon}{\partial E}\right)_{\rho,m} dE. \tag{89}$$

Inserting (89) in Eq. (88) it becomes

$$dP = d\Pi = \left[\chi + \kappa\left(\frac{\partial \varepsilon}{\partial \rho}\right)_{m,E}\right] d\rho + \kappa\left(\frac{\partial \varepsilon}{\partial m}\right)_{\rho,E} dm + \kappa\left(\frac{\partial \varepsilon}{\partial E}\right)_{\rho,m} dE. \tag{90}$$

Considering that

$$\varepsilon = E - \frac{1}{2}\frac{m^2}{\rho},$$

from Eq. (90) the pressure derivatives are easily computed as

$$\Pi_{\rho} = \chi + \tfrac{1}{2}v^2\kappa, \quad \Pi_m = -v\kappa, \quad \Pi_E = \kappa. \tag{91}$$

Inserting then the average values of (91) into Eq. (53) it becomes

$$\Delta P = (\tilde{\chi} + \tfrac{1}{2}\tilde{v}^2\tilde{\kappa})\,\Delta\rho - \tilde{v}\tilde{\kappa}\Delta(\rho v) + \tilde{\kappa}\,\Delta E. \tag{92}$$

From the definition of the total energy per unit volume $\Delta E = \Delta\varepsilon + \frac{1}{2}\Delta(\rho v^2)$ we obtain

$$\Delta P = \tilde{\chi}\,\Delta\rho + \tilde{\kappa}\,\Delta\varepsilon + \tfrac{1}{2}\tilde{\kappa}[\tilde{v}^2\,\Delta\rho - 2\tilde{v}\Delta(\rho v) + \Delta(\rho v^2)]. \tag{93}$$

The last term on the r.h.s. of Eq. (93) vanishes because of Eq. (65), i.e. from the definition of $\tilde{v}$. Finally it becomes

$$\Delta P = \tilde{\chi}\,\Delta\rho + \tilde{\kappa}\,\Delta\varepsilon, \tag{94}$$

as derived in [5]. This linear relation among the pressure derivatives is not sufficient to define the average state.

In order to uniquely define the values of $\tilde{\chi}$ and $\tilde{\kappa}$, Vinokur and Montagné propose a procedure that utilizes the information given by the two thermodynamic states L and R. Integrating Eq. (88) along a straightline path between any two states L and R and using (94), they derive the general relations

$$\tilde{\chi} = \int_0^1 \chi[\varepsilon(t), \rho(t)]\,dt, \tag{95.a}$$

$$\tilde{\kappa} = \int_0^1 \kappa[\varepsilon(t), \rho(t)]\,dt, \tag{95.b}$$

where the parameter t is normalized such that $t_L = 0$ and $t_R = 1$.

Since the exact evaluation of the integrals (95) is, in general, expensive, for practical calculations an approximation is required. In [5] the authors propose finding first some approximations $\hat{\chi}$ and $\hat{\kappa}$ to $\tilde{\chi}$ and $\tilde{\kappa}$ using, for example, the midpoint rule,

$$\hat{\chi} = \chi_M = \chi(\varepsilon_M, \rho_M), \tag{96}$$

where the midpoint state is defined by $\rho_M = (\rho_L + \rho_R)/2$ and $\varepsilon_M = (\varepsilon_L + \varepsilon_R)/2$, or the trapezoidal rule,

$$\hat{\chi} = (\chi_L + \chi_R)/2, \tag{97}$$

or, finally, when the two states L and R are further apart, Simpson's rule,

$$\hat{\chi} = (\chi_L + 4\chi_M + \chi_R)/6 \tag{98}$$

with analogous formulas for $\hat{\kappa}$. Then, they find the values of $\tilde{\chi}$ and $\tilde{\kappa}$ that satisfy (94) and that are closest to the approximate values $\hat{\chi}$ and $\hat{\kappa}$. To accomplish this, they project in the χ–κ plane the point $(\hat{\chi}, \hat{\kappa})$ onto the straight line defined by Eq. (94), first manipulating it to work in the $1/\kappa$–χ/κ plane—in order for the average state to be independent of the arbitrary constant present in the definition of ε—and performing a nondimensionalization by the factor $\hat{s}$. They finally obtain the relations

$$\tilde{\chi} = \frac{D\hat{\chi} + \hat{s}^2\,\Delta\rho\,\delta P}{D - \Delta P\,\delta P} \tag{99}$$

$$\tilde{\kappa} = \frac{D\hat{\kappa}}{D - \Delta P\,\delta P} \tag{100}$$

with

$$\begin{aligned} \delta P &= \Delta P - \hat{\chi}\,\Delta\rho - \hat{\kappa}\,\Delta\varepsilon \\ D &= (\hat{s}\,\Delta\rho)^2 + (\Delta P)^2 \\ \hat{s} &= \hat{\chi} + \overline{\overline{\kappa h}}, \end{aligned} \tag{101}$$

where $\overline{\overline{\kappa h}}$ is evaluated by applying to the product κh the same integration formula used for $\hat{\chi}$ and $\hat{\kappa}$. When either $\Delta\rho$ or $\Delta\varepsilon$ approaches zero the expressions (99) and (100) do not become singular. This can happen when both $\Delta\rho$ and $\Delta\varepsilon$ vanish; however, in the latter case there is no jump and so no problem exists.

The choice of the internal energy per unit volume and the density as independent thermodynamic variables allows us to minimize the number of independent variables that must be averaged. In this case, the Roe-average state $\tilde{u}$ is defined as

$$\tilde{u} = (\tilde{v},\, \tilde{H},\, \tilde{\kappa},\, \tilde{\chi})^{\mathrm{T}}$$

and does not explicitly contain the density or the internal energy, thus eliminating the need to define their averages and remaining closer to the original method of Roe for a perfect gas.

At this point, it may seem that the integration procedure (95) has eliminated the nonuniqueness in the definition of the Roe-average state for a real gas, expressed by the fact that (94) is one equation in two unknowns. In reality, the nonuniqueness still persists and more precisely lies in the choice of the path of integration between the left and right states. The exact integration may be reinterpreted as a "clever" means of defining a couple of values $\tilde{\chi}$ and $\tilde{\kappa}$ that satisfies (ii) and (iv) of Property U simultaneously. In fact, it leads to exactly satisfying (94)—or (53)—and allows for the defined $\tilde{\chi}$ and $\tilde{\kappa}$ to reduce nicely to the pointwise values when the integration limits are approached. However, this couple of values is not unique, as can be immediately seen by changing the path of integration.

The approximate integration, followed by the projection stage, further underlines this concept. The projected couple of values $\tilde{\chi}$ and $\tilde{\kappa}$ arising from the approximate values $\hat{\chi}$ and $\hat{\kappa}$ do not generally coincide with the values coming from the exact integration; this can only happen when the approximate values lie on the perpendicular to the straight line defined by (94) passing through the point given by the exact integration values. However, the approximate integration, followed by the projection stage provides a couple of values $\tilde{\chi}$ and $\tilde{\kappa}$ that again satisfies (ii) and (iv) of Property U. Thus, although the nonuniqueness of the definition of the Roe-average state for an equilibrium real gas still persists, the approximate-integration/projection-stage procedure is a practical means of determining one possible combi-

nation of values $\tilde{\chi}$ and $\tilde{\kappa}$ satisfying Property U. Other combinations can be obtained simply by changing the approximate integration formula.

4.2. Liou *et al.*'s Generalization

In [6, 7] the authors consider an equation of state of the form

$$P = P(e, \rho). \tag{104}$$

Denoting the pressure derivatives with

$$P_e = \left(\frac{\partial P}{\partial e}\right)_\rho, \quad P_\rho = \left(\frac{\partial P}{\partial \rho}\right)_e$$

and following a procedure similar to Eqs. (88)–(90), we find

$$\Pi_\rho = P_\rho + (\tfrac{1}{2}v^2 - e)(P_e/\rho), \quad \Pi_m = -v(P_e/\rho), \quad \Pi_E = (P_e/\rho). \tag{105}$$

Inserting the average values into Eq. (53), it becomes

$$\Delta P = [\tilde{P}_\rho + (\tfrac{1}{2}\tilde{v}^2 - \tilde{e})(\tilde{P}_e/\tilde{\rho})]\,\Delta\rho - \tilde{v}(\tilde{P}_e/\tilde{\rho})\Delta(\rho v) + (\tilde{P}_e/\tilde{\rho})\,\Delta E. \tag{106}$$

Utilizing again the definition of E, we may write

$$\Delta E = \Delta(\rho e) + \tfrac{1}{2}\Delta(\rho v^2), \tag{107}$$

so that Eq. (106) becomes

$$\Delta P = \tilde{P}_\rho\,\Delta\rho + (\tilde{P}_e/\tilde{\rho})[\Delta(\rho e) - \tilde{e}\,\Delta\rho] + \tfrac{1}{2}(\tilde{P}_e/\tilde{\rho})\,\Delta E[\tilde{v}^2\,\Delta\rho - \tilde{v}\Delta(\rho v) + \Delta(v^2)]. \tag{108}$$

The last term on the r.h.s. of Eq. (108) vanishes because of the definition of $\tilde{v}$. The definition of $\tilde{e}$ and $\tilde{\rho}$ is obtained, introducing the additional assumption that the relation

$$\Delta(\rho e) = \tilde{\rho}\,\Delta e + \tilde{e}\,\Delta\rho \tag{109}$$

holds. In order to satisfy (109) one can define

$$\tilde{\rho} = \sqrt{\rho_{\mathrm{L}}\,\rho_{\mathrm{R}}} \tag{110}$$

$$\tilde{e} = \mathrm{Ro}(e), \tag{111}$$

where $\mathrm{Ro}(\cdot)$ is the Roe-average operator defined in (51). In this manner, also $\Delta(\rho v) - \tilde{v}\,\Delta\rho$ in Eq. (72) reduces to $\tilde{\rho}\Delta v$, thus simplifying the expression. One can note that relations (110) and (111) were not necessary for the definition of the average state of Vinokur.

Equation (108) finally becomes

$$\Delta P = \tilde{P}_\rho \, \Delta\rho + \tilde{P}_e \, \Delta e \tag{112}$$

that constitutes the linear constraint between the relevant pressure derivatives $\tilde{P}_\rho$ and $\tilde{P}_e$, as derived in [6, 7].

In order to satisfy Eq. (112), Glaister [6] suggests expressions for $\tilde{P}_\rho$ and $\tilde{P}_e$ that meet it precisely. However, these formulas introduce two artificial states that can lead to a nonphysical average state; furthermore, they can lie outside the region of validity of the equation of state if one uses curve-fits to obtain the properties of the real gas.

To overcome this, Liou *et al.* [7] propose a simple projection technique. They first find two approximate values $\hat{P}_\rho$ and $\hat{P}_e$ to $\tilde{P}_\rho$ and $\tilde{P}_e$, evaluating P_ρ and P_e in the average state $(\tilde{e}, \tilde{\rho})$,

$$\hat{P}_\rho = P_\rho(\tilde{e}, \tilde{\rho}), \quad \hat{P}_e = P_e(\tilde{e}, \tilde{\rho}). \tag{113}$$

Then, after having nondimensionalized equation (112), they project the point $(\hat{P}_\rho, \hat{P}_e)$ over the straight line defined by (112) itself to define unique values for $\tilde{P}_\rho$ and $\tilde{P}_e$. Among the various nondimensionalizations they propose, we chose the one that uses $\hat{P}_\rho$ and $\hat{P}_e$ as scale factors, leading to the formulas

$$\tilde{P}_\rho = \hat{P}_\rho \left(1 + \frac{\hat{P}_\rho \, \Delta\rho \, \delta P^*}{D^*}\right) \tag{114}$$

$$\tilde{P}_e = \hat{P}_e \left(1 + \frac{\hat{P}_e \, \Delta e \, \delta P^*}{D^*}\right), \tag{115}$$

with

$$\delta P^* = \Delta P - \hat{P}_\rho \, \Delta\rho - \hat{P}_e \, \Delta e \tag{116}$$

$$D^* = (\hat{P}_\rho \, \Delta\rho)^2 + (\hat{P}_e \, \Delta e)^2. \tag{117}$$

As for (99)–(100), Eqs. (114)–(115) will become singular only when both $\Delta\rho$ and Δe approaches zero, i.e., when there is no jump.

It is possible to generalize the approach of Liou *et al.*, following Vinokur's idea. Vinokur in [5] reformulates the procedure proposed by Liou *et al.* from the standpoint of defining a unique average state via an integration of the pressure derivatives between the left and right states. Actually, the approximation (113) of the averaged pressure derivatives $\tilde{P}_\rho$ and $\tilde{P}_e$ may be interpreted as an approximation of the evaluation of the weighted integrals of P_ρ and P_e between the L and R states. But in order for the scheme to reduce nicely to Roe's average state for a perfect gas, in the case of an equation of state of the form (104) the integrals analogous to (95) must be written in a slightly different form. As pointed out by Vinokur, the state C defined by $\tilde{\rho}$ and $\tilde{e}$ does not lie on the straight line path connecting states

L and R in the ρ–e plane; one thus has to integrate along the piecewise smooth path L–C–R, instead of the linear path L–R.

The integral formulae which define exactly $\tilde{P}_\rho$ and $\tilde{P}_e$ may be found in [5]. Here we will report only their approximations, analogous respectively to (96)–(98),

$$\hat{P}_\rho = P_\rho(\tilde{e}, \tilde{\rho}), \qquad \hat{P}_e = P_e(\tilde{e}, \tilde{\rho}) \tag{118}$$

$$\hat{P}_\rho = \alpha P_{\rho_L} + (1-\alpha) P_{\rho_R}, \quad \hat{P}_e = (1-\alpha) P_{e_L} + \alpha P_{e_R} \tag{119}$$

$$\hat{P}_\rho = \tfrac{1}{2}[\alpha P_{\rho_L} + P_\rho(\tilde{e}, \tilde{\rho}) + (1-\alpha) P_{\rho_R}] \tag{120.a}$$

$$\hat{P}_e = \tfrac{1}{2}[(1-\alpha) P_{e_L} + P_e(\tilde{e}, \tilde{\rho}) + \alpha P_{e_R}], \tag{120.b}$$

where α is given by

$$\alpha = \frac{\sqrt{\rho_L}}{\sqrt{\rho_L} + \sqrt{\rho_R}}. \tag{121}$$

Once having determined the approximations $\hat{P}_\rho$ and $\hat{P}_e$, one again obtains $\tilde{P}_\rho$ and $\tilde{P}_e$ using relations (114)–(115).

We can summarize the comparison between the approach of Vinokur and Montagné and that of Liou *et al.* by concluding that the choice of e and ρ as independent thermodynamic variables leads to a more complex and thus, in principle, less computationally efficient average state. The Roe-average state $\tilde{u}$ is defined as

$$\tilde{u} = (\tilde{v}, \tilde{H}, \tilde{P}_e, \tilde{P}_\rho, \tilde{e}, \tilde{\rho})^T$$

and forces us to define, besides the usual average quantities, also the average density $\tilde{\rho}$ and the average internal energy $\tilde{e}$. Moreover, formulas (118)–(120) for the approximated averaged pressure derivatives appear to be more complex and from a theoretical standpoint less accurate than the corresponding relations (96)–(98), since the integration path L-C-R is not a straightline path.

However, one can expect the two generalizations to cost approximately the same in terms of CPU-time, since the projection stage of Vinokur is more involved than the one of Liou *et al.*; yet it is constructed on a more solid theoretical basis.

4.3. Cox–Cinnella's Generalization

The formulation proposed by Cox and Cinnella [8–9] is somewhat more difficult to fit in the general framework developed in Section 3. They express all of the thermodynamic variables in terms of temperature and density. Assuming that at equilibrium conditions for a given pair (T, ρ) the chemical composition of the mixture $\{\rho_s\}$ is known, they use Eq. (6) for the pressure, i.e. an equation of state in the form

$$P = P(T, \rho) \tag{122}$$

and relate the speed of sound to an isentropic index $\Gamma = \Gamma(T, \rho)$ as

$$a^2 = \Gamma R T,$$

where R is given by (7) and

$$\Gamma = \gamma^e + \frac{\rho}{RT} \sum_{s=1}^{N_C} \left(\frac{\partial Y_s}{\partial \rho} \right)_T [R_s T - (\gamma^e - 1) e_s] \tag{123}$$

$$\gamma^e = \frac{(\partial h/\partial T)_\rho}{(\partial e/\partial T)_\rho} = 1 + \frac{R + T \sum_{s=1}^{N_C} R_s \left(\frac{\partial Y_s}{\partial T} \right)_\rho}{\sum_{s=1}^{N_C} Y_s c_{v_s} + \sum_{s=1}^{N_C} e_s \left(\frac{\partial Y_s}{\partial T} \right)_\rho}, \tag{124}$$

with $c_{v_s} = c_{v_s}(T)$ representing the species' specific heat at constant volume and $Y_s = \rho_s/\rho$ the species' mass fraction. All of these relations hold pointwise at equilibrium conditions.

To define the Roe-average state, the authors make use of the direct substitution in the eigenvector expansion of Δf and Δu, Eqs. (68)–(69). However, the derivation of the right eigenvectors of the average Jacobian $\tilde{A}$ starting from an equation of state like (122) is very cumbersome, since the temperature is related to the conservative variables m and E only implicitly, through the definition of E and the internal energy equation (13). Actually, the average eigenvector matrix formulated in [8] is

$$\tilde{R} = \frac{\tilde{\rho}}{\sqrt{2}\tilde{a}} \begin{bmatrix} 1 & 1 & 1 \\ \tilde{v} & \tilde{v} + \tilde{a} & \tilde{v} - \tilde{a} \\ \tilde{H} - \dfrac{\tilde{a}^2}{\tilde{\gamma} - 1} & \tilde{H} + \tilde{a}\tilde{v} & \tilde{H} - \tilde{a}\tilde{v} \end{bmatrix}, \tag{125}$$

where $\tilde{\gamma} = \tilde{\gamma}^e$, and implies the use of an equation of state in the form of Eq. (87), as in Vinokur's method. Instead of explicitly considering the average pressure derivatives $\tilde{\kappa}$ and $\tilde{\chi}$, Cox and Cinnella define the average state in terms of $\tilde{\gamma}$ and $\tilde{a}^2$. It may be verified through some thermodynamic derivations that, locally, the following equivalencies hold:

$$\kappa = \gamma^e - 1 \tag{126}$$

$$\chi = a^2 - (\gamma^e - 1)(H - \tfrac{1}{2}v^2). \tag{127}$$

Inserting (126)–(127) in (91) we can obtain the expression of the generalized pressure derivatives in terms of a^2 and γ^e as

$$\Pi_\rho = a^2 - (\gamma^e - 1)(H - v^2), \quad \Pi_m = -(\gamma^e - 1)v, \quad \Pi_E = \gamma^e - 1. \tag{128}$$

We remark that the same result may be achieved by inspection, comparing the eigenvector formulations (125) and (71) that are valid also for a local state, and

considering Eq. (76)—also holding pointwise—and Eq. (45). Accounting for the different normalizations of the eigenvectors (that in [8] appears computationally less efficient, since it requires defining an average density), it is easily deduced that expressions (128) hold pointwise.

Following again the general procedure developed in Section 3, we assume that the relations (128) are valid also for the average state; inserting them into Eq. (53), we have

$$\Delta P = [\tilde{a}^2 - (\tilde{\gamma} - 1)(\tilde{H} - \tilde{v}^2)]\,\Delta\rho - (\tilde{\gamma} - 1)\tilde{v}\Delta(\rho v) + (\tilde{\gamma} - 1)\Delta(\varepsilon + \tfrac{1}{2}\rho v^2)$$

which, considering (65), results in

$$\Delta P = [\tilde{a}^2 - (\tilde{\gamma} - 1)(\tilde{H} - \tfrac{1}{2}\tilde{v}^2)]\,\Delta\rho + (\tilde{\gamma} - 1)\,\Delta\varepsilon \tag{129}$$

that defines the linear relation between $\tilde{\gamma}$ and $\tilde{a}^2$ as formulated in [9], equivalent to (94) and (112). In addition—because of the chosen eigenvector normalization—the authors have to define $\tilde{\rho}$ as in Eq. (110) to satisfy Eqs. (68)–(69).

To deal with the nonuniqueness of the average state, Cox and Cinnella do not try to obtain some approximate values of $\tilde{\gamma}$ and $\tilde{a}^2$ and then correct them to satisfy (129) directly. Instead, they take advantage of having selected T and ρ as independent variables—Eqs. (122)–(124)—and manipulate Eq. (129) so as to formulate it only in terms of the jumps ΔT and $\Delta\rho$. Then they find the expressions of $\tilde{\gamma}$ and $\tilde{a}^2$ that exactly satisfy the resulting transformed relation. This approach may be summarized as follows:

Considering Eqs. (1) and (6), the jumps ΔP and $\Delta\varepsilon$ can be expressed in terms of $\Delta\rho$, ΔT, Δe_s, and $\Delta(\rho_s/\rho)$ through the formulas

$$\Delta P = \tilde{\rho}\tilde{R}\,\Delta T + \tilde{R}\tilde{T}\,\Delta\rho + \tilde{\rho}\tilde{T}\sum_{s=1}^{N_C} R_s\,\Delta Y_s \tag{130}$$

$$\Delta(\rho e) = \tilde{\rho}\sum_{s=1}^{N_C}\tilde{Y}_s\,\Delta e_s + \tilde{\rho}\sum_{s=1}^{N_C}\tilde{e}_s\,\Delta Y_s + \sum_{s=1}^{N_C}\tilde{Y}_s\tilde{e}_s\,\Delta\rho, \tag{131}$$

where $\tilde{\rho}$ is defined by (110) and all of the other average variables are defined by the standard Roe average as

$$\tilde{R} = \mathrm{Ro}(R), \quad \tilde{T} = \mathrm{Ro}(T), \quad \tilde{Y}_s = \mathrm{Ro}(Y_s), \quad \tilde{e}_s = \mathrm{Ro}(e_s). \tag{132}$$

Then, considering the differentials $de_s = c_{v_s}(T)\,dT$ and $dY_s = (\partial Y_s/\partial\rho)_T\,d\rho + (\partial Y_s/\partial T)_\rho\,dT$, one can integrate between the left and the right states with a procedure similar to Vinokur's, obtaining

$$\Delta e_s = \tilde{c}_{v_s}\,\Delta T \tag{133}$$

$$\Delta Y_s = \left(\frac{\partial\tilde{Y}_s}{\partial\rho}\right)_T\Delta\rho + \left(\frac{\partial\tilde{Y}_s}{\partial T}\right)_\rho\Delta T, \tag{134}$$

where $\tilde{c}_{v_s}$, $(\partial \tilde{Y}_s/\partial \rho)_T$, and $(\partial \tilde{Y}_s/\partial T)_\rho$ are defined by means of integral averages [9]. For practical purposes the integrals are approximated, for example, by means of the trapezoidal formula $\bar{c}_{v_s} = [c_{v_s}(T_L) + c_{v_s}(T_R)]/2$, with similar formulas for $\overline{(\partial Y_s/\partial \rho)_T}$ and $\overline{(\partial Y_s/\partial T)_\rho}$, where the bar indicates that these are approximate values. The approximate integral averages are then used directly in (133) and (134), which, substituted into (130) and (131), allow us to express ΔP and $\Delta \varepsilon$ solely in terms of $\Delta \rho$ and ΔT.

Equation (129) thus becomes

$$\left[\tilde{\rho}\sum_{s=1}^{N_C}\tilde{Y}_s\bar{c}_{v_s} + \tilde{\rho}\sum_{s=1}^{N_C}\tilde{e}_s\overline{\left(\frac{\partial Y_s}{\partial T}\right)_\rho} - \frac{\tilde{p}\tilde{R}}{\tilde{\gamma}-1} - \frac{\tilde{p}\tilde{T}}{\tilde{\gamma}-1}\sum_{s=1}^{N_C}R_s\overline{\left(\frac{\partial Y_s}{\partial T}\right)_\rho}\right]\Delta T$$
$$+\left[\sum_{s=1}^{N_C}\tilde{Y}_s\tilde{e}_s + \tilde{\rho}\sum_{s=1}^{N_C}\tilde{e}_s\overline{\left(\frac{\partial Y_s}{\partial \rho}\right)_T} + \frac{\tilde{\chi}-\tilde{p}\tilde{T}}{\tilde{\gamma}-1} - \frac{\tilde{p}\tilde{T}}{\tilde{\gamma}-1}\sum_{s=1}^{N_C}R_s\overline{\left(\frac{\partial Y_s}{\partial \rho}\right)_T}\right]\Delta\rho = 0, \qquad (135)$$

where $\tilde{\chi} = \tilde{a}^2 - (\tilde{\gamma}-1)(\tilde{H} - \frac{1}{2}\tilde{v}^2)$.

Since the variations $\Delta\rho$ and ΔT are independent, Eq. (135) is satisfied if and only if the two coefficients in brackets simultaneously vanish. They represent two equations in terms of the two unknowns $\tilde{\gamma}$ and $\tilde{a}^2$, which are then given by

$$\tilde{\gamma} = 1 + \frac{\tilde{R} + \tilde{T}\sum_{s=1}^{N_C}R_s\overline{\left(\frac{\partial Y_s}{\partial T}\right)_\rho}}{\sum_{s=1}^{N_C}\tilde{Y}_s\bar{c}_{v_s} + \sum_{s=1}^{N_C}\tilde{e}_s\overline{\left(\frac{\partial Y_s}{\partial T}\right)_\rho}} \qquad (136)$$

$$\tilde{a}^2 = \tilde{\Gamma}\tilde{R}\tilde{T} + (\tilde{\gamma}-1)\left(\tilde{H} - \tfrac{1}{2}\tilde{v}^2 - \sum_{s=1}^{N_C}\tilde{Y}_s\tilde{e}_s - \tilde{R}\tilde{T}\right), \qquad (137)$$

where for convenience an average Γ has been introduced:

$$\tilde{\Gamma} = \tilde{\gamma} + \frac{\tilde{p}}{\tilde{R}\tilde{T}}\sum_{s=1}^{N_C}\overline{\left(\frac{\partial Y_s}{\partial \rho}\right)_T}[R_s\tilde{T} - (\tilde{\gamma}-1)\tilde{e}_s]. \qquad (138)$$

The average state is then completely defined. One should note, however, that the nonuniqueness of the definition of the average state still persists and in this case lies in the choice of the integration path in the definition of $(\partial \tilde{Y}_s/\partial \rho)_T$ and $(\partial \tilde{Y}_s/\partial T)_\rho$. One can also observe that the previous relations do not become singular in smooth regions and are consistent with the original Roe-average state in the limit of a perfect-gas behavior of the mixture.

This approach, however, does not satisfy Eq. (129) exactly, since the approximations used to compute $\tilde{c}_{v_s}$, $(\partial \tilde{Y}_s/\partial \rho)_T$, and $(\partial \tilde{Y}_s/\partial T)_\rho$ introduce an error in the expressions of the jumps ΔP and $\Delta \varepsilon$ as functions of $\Delta\rho$ and ΔT, which are used in the definition of $\tilde{\gamma}$ and $\tilde{a}^2$. Consequently, Eq. (47) is not exactly satisfied. This inaccuracy is not cured by performing a projection stage upon relation (134). In order to exactly express ΔP and $\Delta \varepsilon$ in terms of $\Delta\rho$ and ΔT the only acceptable

values for $(\partial \tilde{Y}_s/\partial \rho)_T$ and $(\partial \tilde{Y}_s/\partial T)_\rho$ are those that exactly meet the integral averages and not any combination of them satisfying (134).

To fix this, a projection stage similar to Vinokur's can be performed. Since the values of $\tilde{\gamma}$ and $\tilde{a}^2$, given by (136)–(137) do not meet (129) precisely (as happens in (94) with the values $\hat{\chi}$ and $\hat{\kappa}$), they may consequently be indicated as $\hat{\gamma}$ and $\hat{a}^2$ and recast in terms of $\hat{\chi}$ and $\hat{\kappa}$ through the formulas

$$\hat{\chi} = \hat{a}^2 - (\hat{\gamma} - 1)(\tilde{H} - \tfrac{1}{2}\tilde{v}^2) \tag{139}$$

$$\hat{\kappa} = \hat{\gamma} - 1. \tag{140}$$

One may then project them onto the straight line (129), or (94), using Eqs. (99)–(103), with $\hat{s}$ taken as $\hat{s} = \hat{a}^2$. The resulting couple of values $\tilde{\chi}$ and $\tilde{\kappa}$ finally defines $\tilde{\gamma}$ and $\tilde{a}^2$ satisfying Eq. (129), and thus (47), precisely.

We may assume that recasting the pressure derivatives in terms of the two "gammas" and a^2 is due mainly to two reasons. The first relies on the willingness of using T and ρ as independent thermodynamic variables, which allows us to immediately couple the Riemann solver with the "black box" solver [15] that Cinnella and Cox developed to compute the thermochemical state; in fact, after having determined the chemical composition, the derivatives in terms of T and ρ are easily obtained. The second reason is given by the fact that this framework, explicitly containing the chemical species, is compatible with the extension to the more general nonequilibrium case.

However, if one is mainly interested in equilibrium simulations, one does not necessarily need to directly introduce in the flow solver the information given by the knowledge of the chemical composition. With a proper definition of the average state, the thermochemical solver can be kept separated and utilized only to evaluate the pressure derivatives, the enthalpy, and all of the other needed thermodynamic quantities, as can be done with the previous methods [5, 7]. Keeping the chemistry separated from the flow solver, the latter may be coupled either to a correct determination of thermodynamic properties or to a simple curve-fit evaluation of them. From this standpoint, the present approach appears to be more restrictive than the previous ones, while the evaluation of the average state,

$$\tilde{w} = \left(\tilde{v}, \tilde{H}, \tilde{\gamma}, \tilde{a}^2, \tilde{e}, \tilde{\rho}, \tilde{R}, \tilde{T}, \tilde{e}_s, \tilde{Y}_s, \tilde{c}_{v_s}, \left(\frac{\partial \tilde{Y}_s}{\partial T}\right)_\rho, \left(\frac{\partial \tilde{Y}_s}{\partial \rho}\right)_T \right)^{\mathrm{T}},$$

requires the computation of a larger number of thermodynamic variables, both in the thermochemical procedure and in the averaging process itself, thus appearing less efficient.

5. NUMERICAL TESTS

In this section we will test the solvers previously described, which will be respectively referred to as Vinokur's, Liou's, and Cinnella's solver. All the results reported are obtained with the second-order symmetric TVD scheme of Yee [12]; in the

following the second minmod limiter function proposed in [12] is always utilized. The main interest here is in comparing the features of the different solvers on some steady flows and not in accelerating convergence to steady state. Thus, a simple explicit time integration scheme is utilized, using the free-stream values as the initial condition and letting the solution evolve at a constant time step until steady state is reached.

The sonic entropy fix is carried out by means of the approach of Harten and Hyman [22], while the stability for the hypersonic case is enhanced as proposed by Yee [12]. It is well known (see, for example, [23, 24]) that in the supersonic regime, depending upon the asymptotic conditions and the mesh adopted, Roe's scheme often leads to unpredictable nonphysical solutions; thus, in these cases a fix is necessary.

One-dimensional tests for Vinokur's and Liou's solvers, using curve-fits for equilibrium air property evaluations, are widely reported in [11, 7], where it is shown that these solvers are capable of giving good results in one space dimension even under extreme initial conditions. Here we will restrict our attention to the more realistic 2D case in order to show that these solvers, as well as Cinnella's, are able to predict 2D flows. We also show that all of them may be efficiently coupled to the procedure we developed for the exact thermochemical air property evaluations.

The first test case (Test Case 1) we consider is a 2D blunt body calculation. The body geometry and the free stream conditions are those proposed in [8], where it is considered a blunt 9° half-angle cone flying at $M_\infty = 10$, at zero angle of attack and at an altitude of approximately 10 km, where the pressure is $P_\infty = 26.5 \times 10^3$ Pa, the density $\rho_\infty = 0.414$ kg/m^3, and the temperature $T_\infty = 223$ K. In Test Case 1 a 70×20 grid is employed (Fig. 5), where the grid centerline is treated as a wall boundary; the time step utilized is 0.6×10^{-5} s, corresponding to a Courant number approximately equal to 0.65, the maximum value by which the solution is able to reach convergence.

Test Case 1 was run with both Vinokur's and Liou's solvers combined for all the three proposed integration formulas and with Cinnella's solver. The solvers were also experimented with all of the proposed air mixtures, while only Vinokur's and Liou's used the curve-fits of Scrinivasan [14]. The steady state solution results were the same for all of the combinations of solvers and air mixtures experienced. Using, instead, the curve-fits with Vinokur's and Liou's solvers, the results differ slightly because of the different mixture composition used for interpolating air properties and probably because of the limited accuracy of the fits themselves, too. Cinnella's solver was able to converge to the steady state even without the projection stage, although the corresponding steady solution result was slightly different; instead, the calculations with Vinokur's and Liou's solvers blew up if the projection stage was switched off. This suggests that the procedure followed in the definition of the average state of Cinnella and Cox leads to a couple of independent variables ($\tilde{a}^2$ and $\tilde{\gamma}$, instead of the two pressure derivatives) that better meets Eq. (53) when their values are approximate.

A summary of the results obtained in the various cases is presented in Table I. In Fig. 6 the density isolines for Vinokur's solver (trapezoidal rule, AM1) are shown, while in Fig. 7 the temperature distribution along the stagnation line and the body

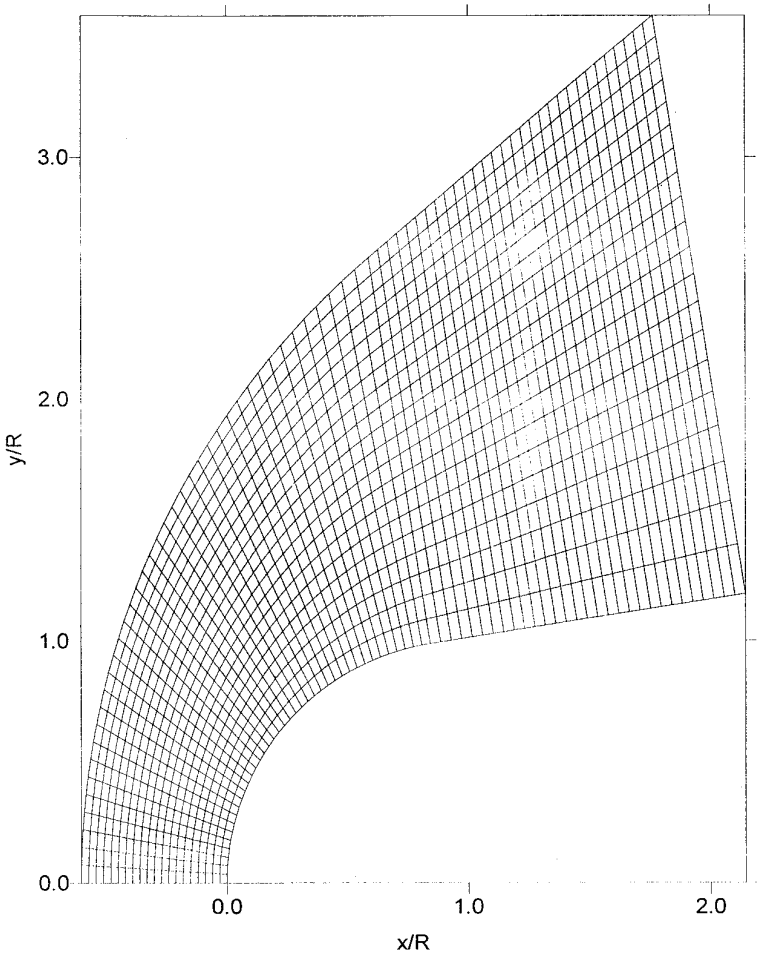

FIG. 5. 70×20 grid for Test Case 1.

surface for both equilibrium air and perfect gas is reported. Finally, in Fig. 8 the molar fraction distribution (AM1) is presented. The quality of the solution is good, as one can note, observing that the shock is captured in very few cells, even if the grid of Test Case 1 is relatively coarse. In particular, where the solution is aligned with the grid, the shock is spread over two cells at most. This is typical of Roe's scheme, since it exactly satisfies the jump conditions at each interface.

Both temperature and molar fraction distribution are in good agreement with those of [8]. In particular, the computed stagnation temperature is approximately 3518 K, which explains why, using different air mixtures, the results are unchanged. The temperature is sufficiently low so that the formation of ionized species has not yet begun; thus, AM1 gives results that are sufficient to provide accurate equilibrium air properties in this test case.

Comparisons between convergence histories are reported in Figs. 9–12, in terms of the maximum nondimensionalized residual among the four conservative variables against CPU-time (an HP series 735 workstation was utilized). A comparison be-

TABLE I
Summary of Results for Test Case 1 and Test Case 2

	Test Case I		Test Case II	
	T_{st}/T_∞	CPU-time (s)	T_{st}/T_∞	CPU-time (s)
Perfect gas.	21.15	402	—	—
Vin. trap. (AM1)	15.77	1428	23.57	4086
Vin. trap. (AM2)	15.77	1736	23.56	5096
Vin. trap. (AM3)	15.77	2739	23.56	8099
Vin. midp. (AM1)	15.77	3462	23.57	10351
Vin. Simp. (AM1)	15.77	3310	23.57	10383
Vin. trap. (fits)	15.59	577	23.39	1806
Liou trap. (AM1)	15.77	1412	23.57	4138
Liou midp. (AM1)	15.77	3306	23.57	10347
Liou Simp. (AM1)	15.77	3320	23.57	10483
Cinn. trap. (AM1)	15.77	1613	23.57	4834

tween the three approximate integration formulas with Vinokur's solver coupled to AM1 can be found in Fig. 9. Convergence is reached for all three approximate formulas, which showed to be equally robust in this test case, although in the case of midpoint and Simpson's rules the computational effort is significantly higher. This is partially due to the higher number of iterations (not reported) necessary to reach the same residual with respect to the case of trapezoidal rule. However, the main reason lies in the fact that, using these formulas, the Euler solver must call the thermochemical procedure for each cell at each time iteration one more time than in the case of the trapezoidal rule. The same comparison over the three approximate formulas is carried out, in the case of Liou's solver, in Fig. 10; the overall behavior is the same as in the case of Vinokur's solver. It may be noted that the usage of the trapezoidal rule significantly improves the efficiency of the original Liou's method, where only the midpoint rule was considered.

In order to evaluate the differences in computational time required by the use of the different air mixtures, the convergence histories for Vinokur's solver with the trapezoidal rule coupled to the three proposed air models are presented in Fig. 11. One can note that the curves are almost the same, only shifted toward increasing times as the complexity of the air mixture considered increases. As already mentioned, in this test case the dissociation is still far from the ionized species formation

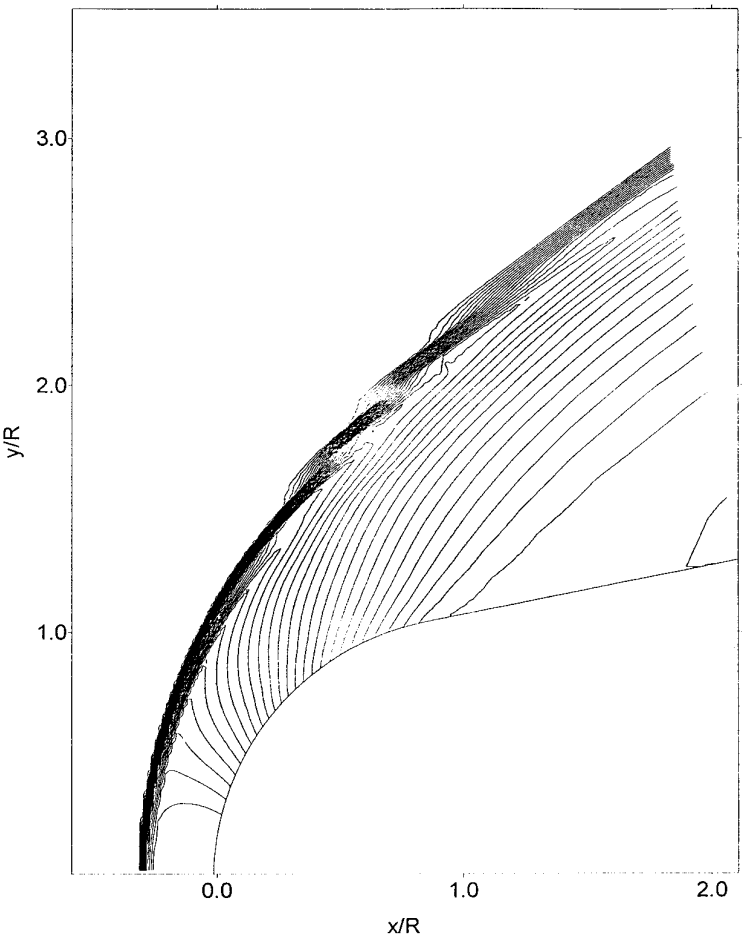

FIG. 6. Test Case 1: density isolines, $\Delta\rho = 0.1$ kg/m^3, using Vinokur's solver (trapezoidal rule, AM1).

threshold, so that the thermochemical procedure gives almost the same results using different models. As expected, the use of AM3 results in the highest computational effort.

The convergence histories obtained by means of the three solvers coupled to the trapezoidal rule using AM1 are reported in Fig. 12; the residual histories of the perfect gas and curve-fit models are also presented. The aim here is to compare the three solvers over the same conditions and to assess the increase in computational cost in equilibrium calculations with respect to the use of the perfect gas model. The convergence histories confirm what was expected from the discussion of Section 4: while Vinokur's and Liou's solvers behave approximately the same, Cinnella's requires a higher computational effort, because of the higher number of functional evaluations needed to obtain the average state.

The use of Vinokur's and Liou's solvers with the trapezoidal rule, coupled to the exact determination of equilibrium air properties by means of AM1, requires

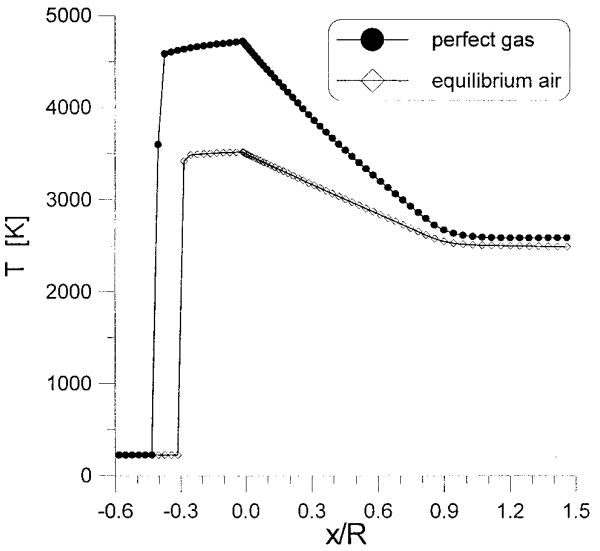

FIG. 7. Temperature distribution along the stagnation line and surface; comparison between perfect gas and equilibrium air (Test Case 1: Vinokur's solver, trapezoidal rule, AM1).

approximately three times the computational time necessary to the perfect gas model. Equilibrium calculations based upon curve-fit evaluation of the thermodynamic properties requires, of course, less extra time, but they are not always robust enough to guarantee convergence and with increasing temperature their accuracy deteriorates. Moreover, they are restricted to one specific mixture composition per tabulation. Yee [12] also notes that the use of curve-fits may lead to the computation

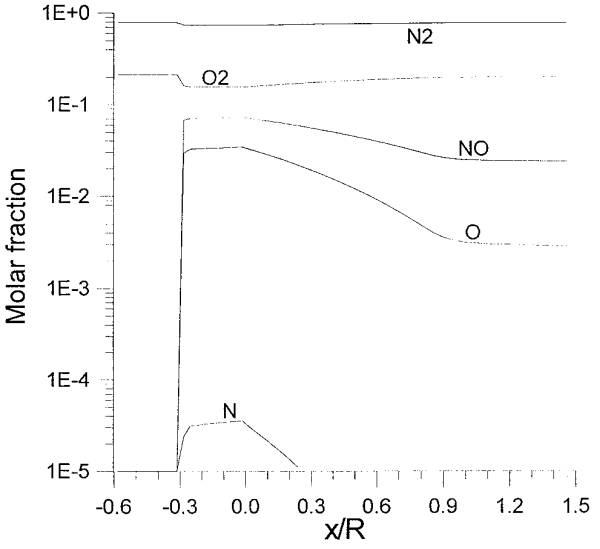

FIG. 8. Molar fraction distribution along the stagnation line and surface (Test Case 1: Vinokur's solver, trapezoid rule, AM1).

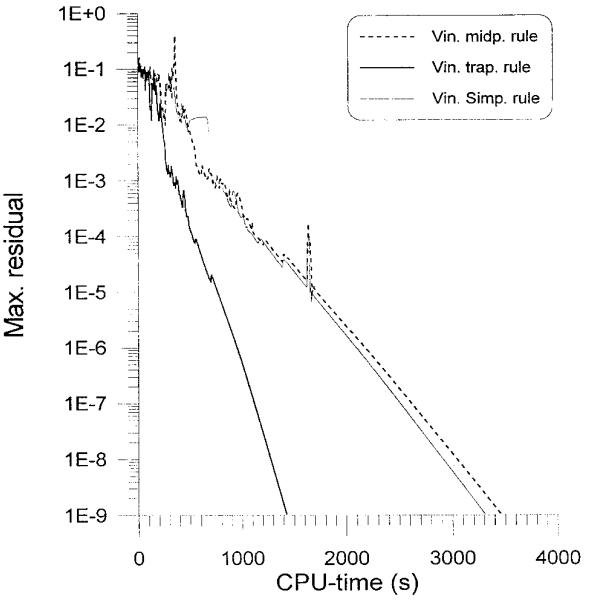

FIG. 9. Maximum residual versus CPU-time using Vinokur's solver and AM1; comparison of different integration formulas (Test Case 1).

of nonphysical average states, characterized by a negative squared speed of sound; while using a simple correction [12] is often possible to fix the problem, this results in an alteration of the time-evolution consistency, negatively affecting the transient to steady state and, thus, the convergence rate. Our experience confirms these

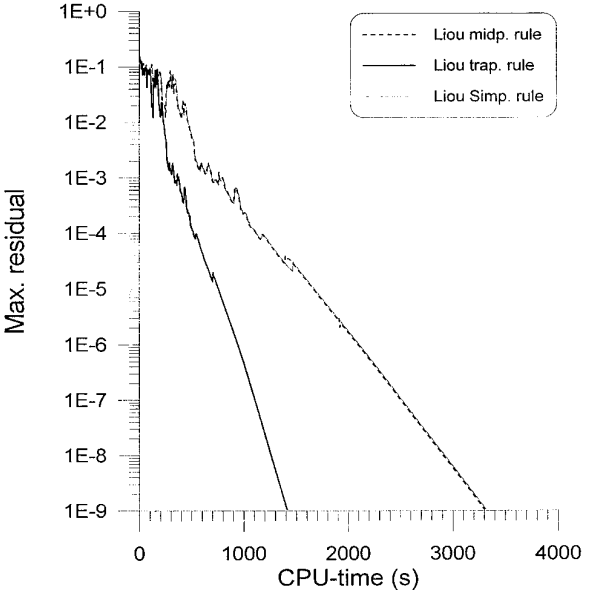

FIG. 10. Maximum residual against CPU-time using Liou's solver and AM1; comparison of different integration formulas (Test Case 1).

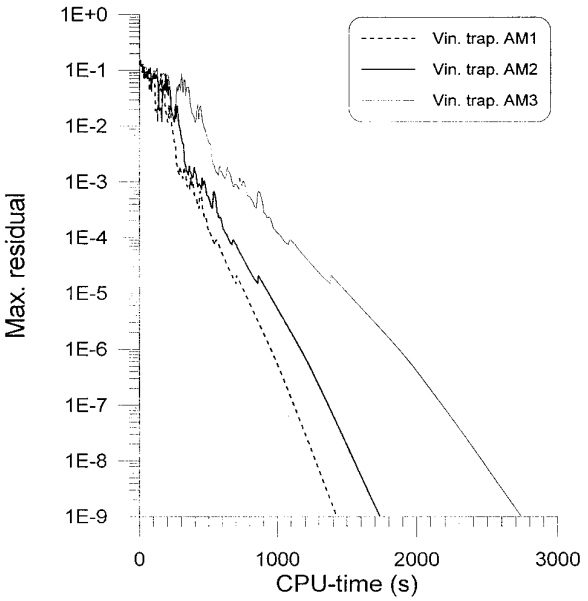

FIG. 11. Maximum residual versus CPU-time using Vinokur's solver and trapezoidal rule; comparison among different air mixtures (Test Case 1).

results; moreover, we have found that convergence problems due to nonphysical average states may be encountered also using the thermochemical procedure. However, because the thermodynamic state computed by means of the chemical composition determination is more accurate than the one obtained using curve-fits, in

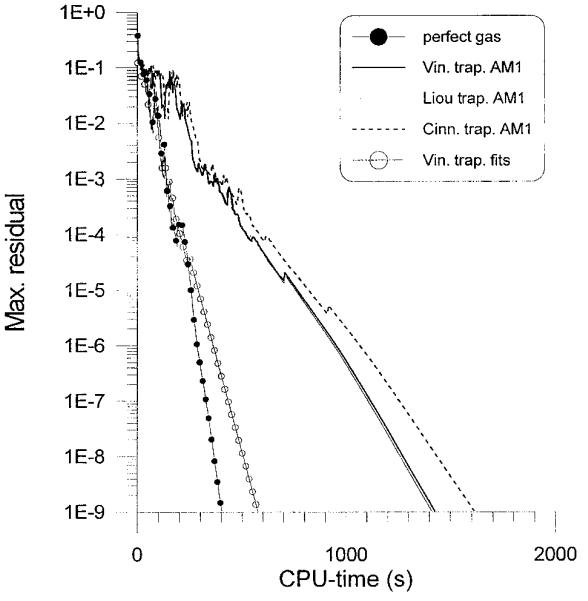

FIG. 12. Maximum residual versus CPU-time using different solvers (trapezoidal rule) and air models (Test Case 1).

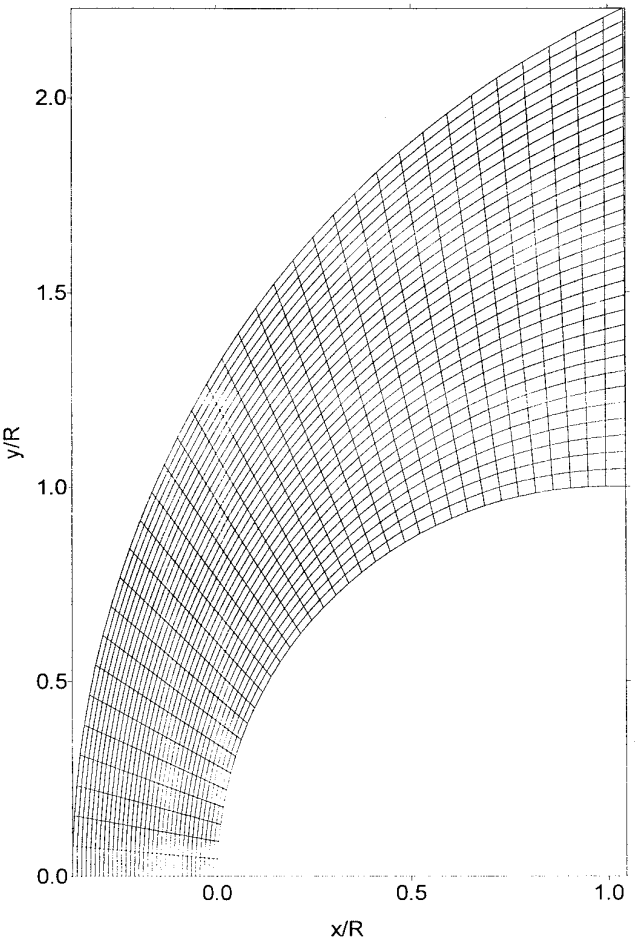

FIG. 13. 72 × 33 grid for Test Case 2.

practice this behavior is less likely to occur using our thermodynamic procedure. Thus, it is found to be generally more robust and accurate to perform equilibrium computations by means of the exact determination of the thermodynamic properties; in Fig. 12 it is shown that this can be done with an acceptable increase of CPU-time.

The second case we tested (Tese Case 2) is the 2D blunt body computation proposed in [12]. The free stream conditions are $M_\infty = 15$, $P_\infty = 1220$ Pa, $\rho_\infty = 0.0188$ kg/m^3, and $T_\infty = 301$ K. In this case a 72 × 33 grid is employed (Fig. 13), where the grid centerline is treated as a wall boundary. The time step utilized is 0.7×10^{-6} s, corresponding to a Courant number approximately equal to 0.3, the maximum value by which the solution is able to reach convergence. Moreover, it has been necessary to utilize the entropy correction of Yee [12] with $\tilde{\delta}_i = 0.15$, $i = 1, ..., 4$, in order to avoid nonphysical solutions.

The density isolines for Vinokur's solver, coupled to the trapezoidal rule and AM1, are presented in Fig. 14. Again, using different integration formulas for Vinokur's and Liou's solvers, the final solution is the same, even if the asymptotic

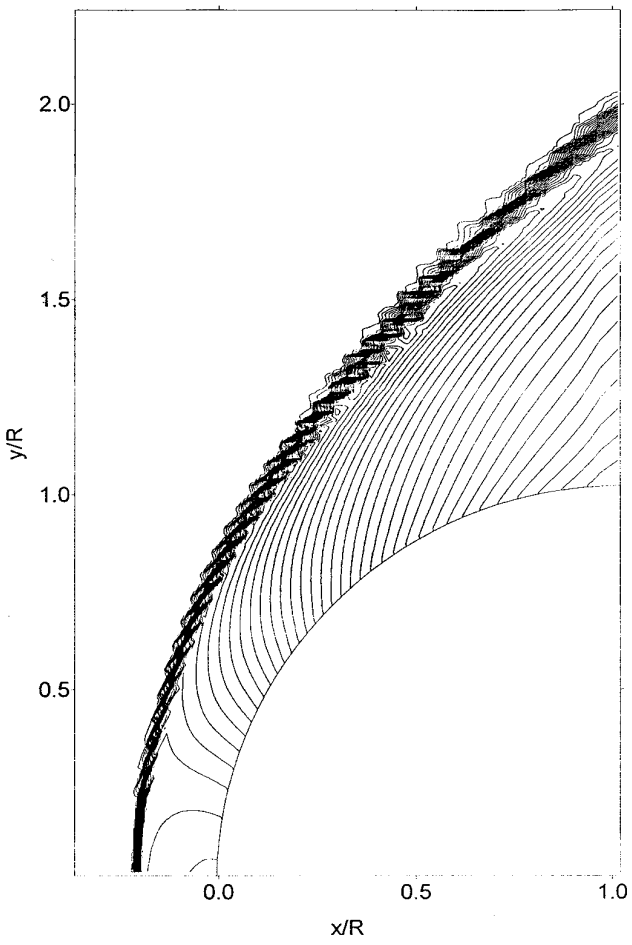

FIG. 14. Test Case 2: density isolines, $\Delta\rho = 0.1$ kg/m^3, using Vinokur's solver (trapezoidal rule, AM1).

conditions are more severe and, consequently, the jump through the shock wave is stronger. Examining also the results in Table I, it can be concluded that the simple trapezoidal integration rule, coupled with the projection techniques developed in [5, 7], is accurate enough to satisfy the constraint on the average pressure derivatives and is to be preferred for its higher efficiency, even in very high Mach number regimes.

In this test case, even with Cinnella's solver the computation blows up when running without projection, while performing the projection stage leads again to a steady state solution equal to those of Vinokur's and Liou's solvers. Thus, in this case all of the solvers present a lack of robustness when the projection stage is switched off.

The use of different chemical models does not significantly alter the final results also in this test case, even if the effect of the different air mixtures begins to become evident (see Table I). In fact, the combination of values of the asymptotic Mach number and altitude is just at the beginning of the region where the effects of AM2

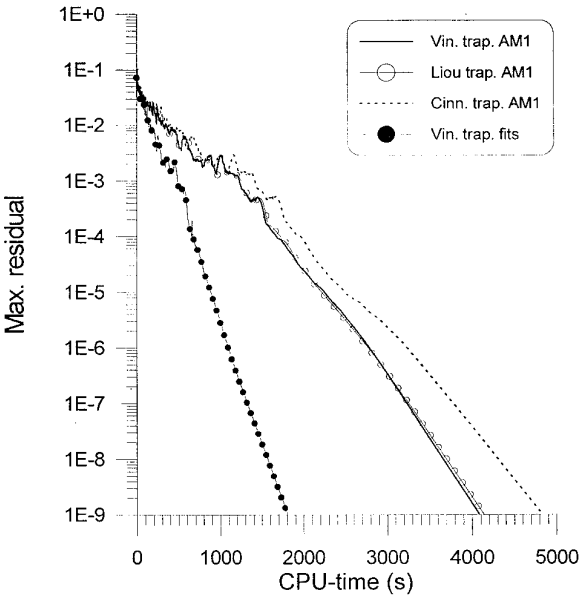

FIG. 15. Maximum residual versus CPU-time using different solvers (trapezoidal rule) and air models (Test Case 2).

over AM1 become important [1]. Again, AM1 is sufficient to provide accurate results. In order to show the different behavior of the various air mixtures it would be necessary to consider a case at a higher Mach number and altitude; here we just want to underline the fact that all the proposed air mixtures are able to provide accurate results in the cases considered.

A comparison among the convergence histories of Vinokur's, Liou's, and Cinnella's solvers with AM1 and Vinokur's with the curve-fits (all with the trapezoidal rule) is presented in Fig. 15. One can note that Vinokur's and Liou's solvers again behave approximately the same, and the use of AM1 instead of the fits requires about twice the computational effort.

The third case (Test Case 3) we consider is a hypersonic flow over a double ellipse geometry, typical of re-entry shuttles' forebody. The free stream conditions are: $M_\infty = 10$, zero angle of attack, and approximately 50 km of altitude, where $P_\infty = 87.05$ Pa, $\rho_\infty = 1.074\ 10^{-3}$ kg/m^3, and $T_\infty = 282.3$ K. We have run Vinokur's, Liou's, and Cinnella's solvers (trapezoidal rule, AM1) over the 165×35 grid reported in Fig. 16, starting again from free stream conditions, until the residual has been reduced of several orders of magnitude. The aim here is to present a computation with the three solvers over a more realistic configuration. We used only the trapezoidal rule, since we previously assessed that it is sufficient in most practical cases. Cinnella's solver was run without a projection stage.

The density isolines computed with Vinokur's solver (trapezoidal rule, AM1) are presented in Fig. 17. The shock appears well resolved even in the regions where the grid is relatively coarse; in particular, the bow and secondary shock interaction is well captured. Temperature distributions along the stagnation line and body

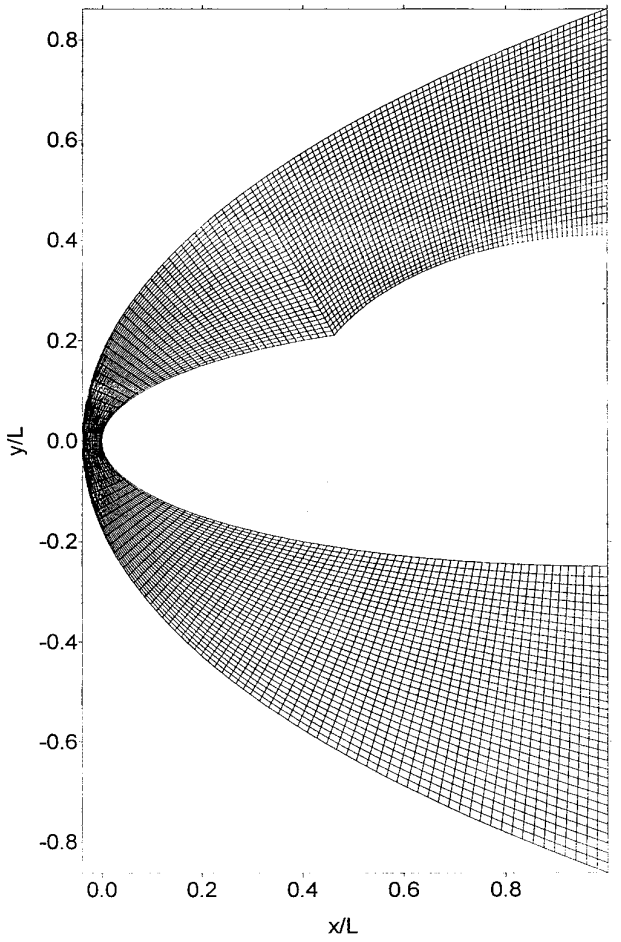

FIG. 16. 165 × 35 grid for Test Case 3.

surface are reported in Fig. 18, where a comparison between the perfect gas and the equilibrium air is carried out. One can note that T_{st}/T_{∞} is lower for the dissociating air and that, after the bow shock, the decrease in temperature is stronger for the perfect gas, since for dissociating air the partial reaggregation of molecules frees energy.

The results obtained using the three solvers are almost identical, even if in this test case the residual with Vinokur's and Liou's solver does not reach machine zero (Fig. 19); the maximum temperature is about 3288 K, which again justifies the use of AM1. In this test case a comparison on the efficiency of the three solvers is not easy to carry out. Vinokur's and Liou's solvers initially appear to be more efficient than Cinnella's solver, but after a residual reduction of four orders of magnitude, their residual histories start to converge at a slower rate than the one of Cinnella and eventually they start to oscillate. However, we can conclude that Vinokur's and Liou's solvers again require less computational time, at least until their residuals reach the value 10^{-4}. One can observe that the computational cost for Vinokur's and Liou's solver is again about the same.

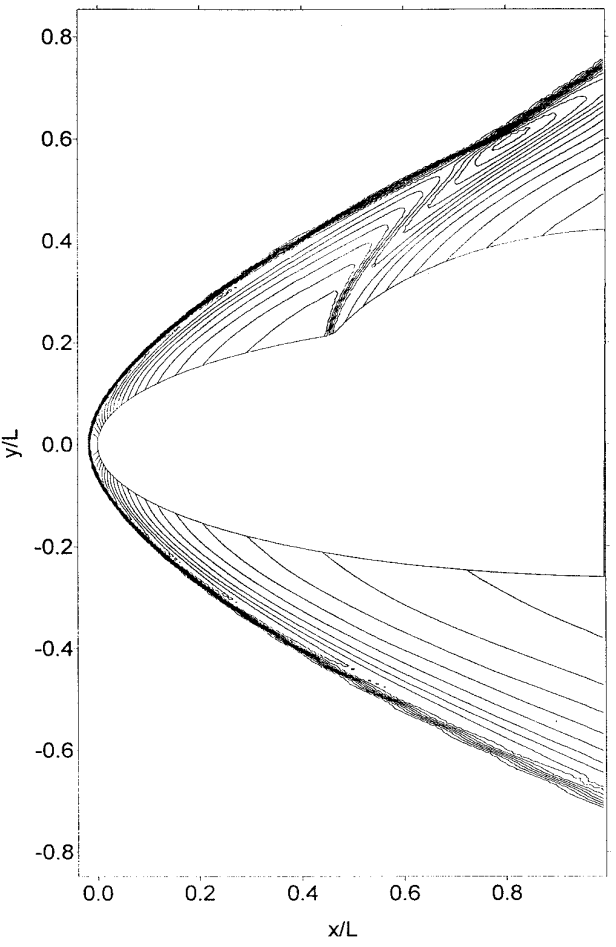

FIG. 17. Double ellipse forebody: density isolines, $\Delta\rho = 0.0005$ kg/m^3, using Vinokur's solver (trapezoidal rule, AM1) (Test Case 3).

6. CONCLUSIONS

In this work, we have first proposed a procedure for the evaluation of the thermochemical properties of air at equilibrium conditions that is efficient and robust. It proved to achieve the correct thermophysical state starting from virtually any initial guess of mixture temperature and composition for every pair of internal energy and density values of practical interest. Moreover, when coupled to any proposed generalized Roe's approximate Riemann solver, it allows equilibrium calculations at an acceptable extra time with respect to perfect gas simulations or to the use of curve-fits.

The extension of Roe's approximate Riemann solver to equilibrium real gas has then been carried out by means of a general formulation. This theoretical framework has allowed us: (i) to prove that the choice of the algebraic technique used to define the Roe-average state does not influence the formal definition of the average state itself, nor its inherent nonuniqueness; (ii) to review some of the existing

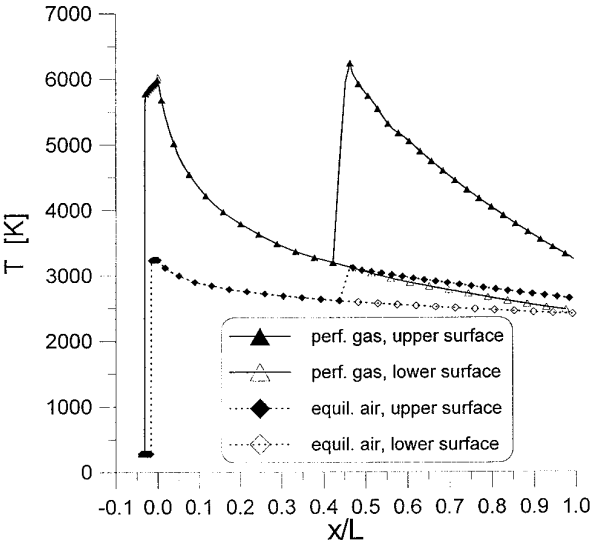

FIG. 18. Temperature distribution along the stagnation line and surface: comparison between perfect gas and equilibrium air (Vinokur's solver, trapezoidal rule, AM1) (Test Case 3).

generalizations of Roe's scheme, namely those by Vinokur and Montagné [5], Liou *et al.* [7], and Cox and Cinnella [8]. The analysis has allowed us to ascertain the influence of the functional form of the equation of state on the average state definition. The choice of internal energy per unit volume and density as independent

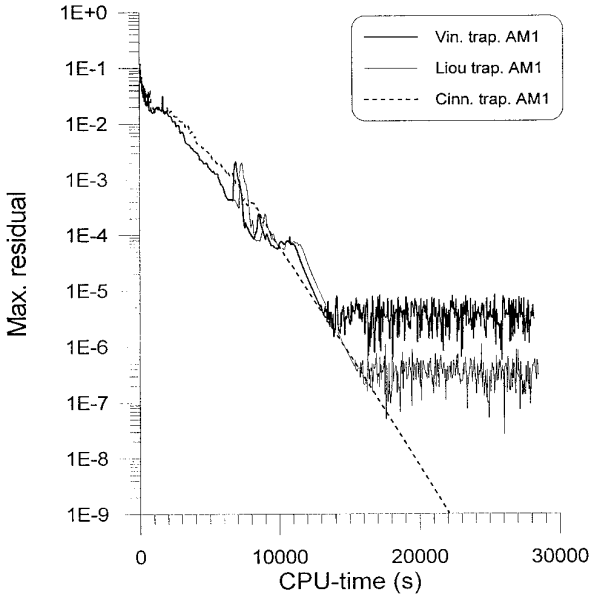

FIG. 19. Maximum residual versus CPU-time using different solvers (trapezoidal rule, AM1) (Test Case 3).

thermodynamic variables is more efficient, since it minimizes the number of average variables to be defined. In Section 4, the different approaches developed to deal with the nonuniqueness of the average state have been described; the projection techniques proposed in [5, 7] are very similar, as confirmed by the numerical results. Moreover, the projection technique of [5] has been extended to the average state of [8], which has then provided numerical results equivalent to those of [5, 7].

The necessity for the projection stage in the analyzed solvers has been assessed from numerical tests. Its presence allows for a definition of the average state that meets all of the requirements of Property U, thus guaranteeing robustness in equilibrium computations based on Roe's scheme, without significantly increasing the CPU-time, and providing for more accurate results.

The numerical performances of the selected solvers have been assessed by means of some 2D numerical tests over typical hypersonic configurations. The equilibrium simulations with any of the evaluated solvers have been shown to be by no means less robust than the perfect gas ones. In the numerical tests presented, the influence of the kinetic model used to represent the air mixture has been found to be negligible. The simpler air mixture proposed in Section 1 (AM1) appears sufficient in providing accurate thermodynamic properties of dissociating air. There are, however, equilibrium regimes where a more sophisticated air model is required. We showed that computations with the proposed AM2 and AM3 are equally robust, although computationally more expensive, because of the increasing complexity of the mixture.

As far as numerical efficiency is concerned, we can conclude that Vinokur's and Liou's solvers behave essentially the same, despite the formal different choice of independent thermodynamic variables, which leads to a different definition of the generalized Roe-averaged state. In the evaluation of the average pressure derivatives it is generally sufficient to resort to an approximate integration by the trapezoidal rule, followed by the projection stage. This results in the smallest computational effort. The use of a more accurate integration, like Simpson's approximate formula, does not appear necessary to better evaluate the average state and, hence, to help convergence.

When comparing either Vinokur's or Liou's solver with Cinnella's, the latter is slightly more expensive than the former. Since Cinnella's solver takes explicitly into account the dependence of the average state on the thermochemical conditions of the right and left states, it makes computationally more expensive the determination of the average state itself. In addition, Vinokur's and Liou's approaches maintain the chemical information separated from the Euler solver, thus allowing the choice of using either a correct and a more robust evaluation of the thermodynamic properties of equilibrium air via chemical composition evaluation or some curve-fits.

ACKNOWLEDGMENTS

The authors are indebted with one of the reviewers for his stimulating criticism and suggestions. They also thank Professor L. Quartapelle for many useful discussions and much advice during the revision of the paper.

REFERENCES

1. R. Gupta, J. Yos, R. Thompson, and K. Lee, NASA RP-1232, 1990.
2. J. A. Desideri, N. Glinsky, and E. Hettena, *Comput. & Fluids* **18,** 151 (1990).

3. V. Selmin and L. Formaggia, *Int. J. Numer. Methods Eng.* **34,** 569 (1992).
4. B. Grossmann and R. W. Walters, *AIAA J.* **27,** 524 (1989).
5. M. Vinokur and J. L. Montagné, *J. Comput. Phys.* **89,** 276 (1990).
6. P. Glaister, *J. Comput. Phys.* **74,** 382 (1988).
7. M.-S. Liou, B. van Leer, and J.-S. Shuen, *J. Comput. Phys.* **87,** 1 (1990).
8. C. F. Cox and P. Cinnella, *AIAA J.* **32,** 519 (1994).
9. C. F. Cox, Ph.D. thesis, Mississippi State University, 1992.
10. R. Abgrall, *Comput. & Fluids* **19,** 171 (1991).
11. J.-L. Montagné, H. C. Yee, and M. Vinokur, *AIAA J.* **27,** 1332 (1989).
12. H. C. Yee, G. H. Klopfer, and J. L. Montagné, *J. Comput. Phys.* **88,** 31 (1990).
13. P. L. Roe, *J. Comput. Phys.* **43,** 357 (1981).
14. S. Scrinivasan, J. C. Tannehill, and K. J. Weilmuenster, NASA CR181245, 1986.
15. P. Cinnella and C. Cox, AIAA Paper 91-3322, 1991.
16. W. C. Vincenti and C. H. Kruger Jr., *Introduction to Physical Gas Dynamics* (Krieger, Melbourne, FL, 1965).
17. C. Park, *Nonequilibrium Hypersonic Aerothermodynamics* (Wiley-Interscience, New York, 1990).
18. D. R. Stull and H. Prophet, *JANAF Thermochemical Tables,* 2nd ed. (National Bureau of Standards, Washington, DC, 1971).
19. P. Cinnella and C. F. Cox, *Comput. Fluid Dyn. J.* **1,** 143 (1992).
20. K. Meintjes and A. P. Morgan, *Comb. Sci. Technol.* **68,** 35 (1989).
21. L. Mottura and M. Zaccanti, thesis, Politecnico di Milano, 1995. [Italian]
22. A. Harten and J. M. Hyman, *J. Comput. Phys.* **50,** 235 (1983).
23. H. C. Lin, *J. Comput. Phys.* **117,** 20 (1995).
24. M.-S. Liou and C. J. Steffen, Jr., *J. Comput. Phys.* **107,** 23 (1993).